Accepted manuscript doi:
10.1680/jgein.18.00009

**Submitted:** 28 June 2017

**Published online in 'accepted manuscript' format:** 19 January 2018

**Manuscript title:** Rubber Powder–Polymer Combined Stabilization of South Australian Expansive Soils

**Authors:** A. Soltani[1], A. Deng[1], A. Taheri[1] and M. Mirzababaei[2]

**Affiliations:** [1]School of Civil, Environmental and Mining Engineering, The University of Adelaide, Adelaide, SA 5005, Australia; [2]School of Engineering and Technology, Central Queensland University, Melbourne, VIC 3000, Australia

**Corresponding author:** A. Soltani, School of Civil, Environmental and Mining Engineering, The University of Adelaide, Adelaide, SA 5005, Australia.

**E-mail:** Amin.Soltani@adelaide.edu.au

Accepted manuscript doi:
10.1680/jgein.18.00009

## ABSTRACT

This study examines the combined capacity of rubber powder inclusion and polymer–treatment in solving the swelling problem of South Australian expansive soils. The rubber powder was incorporated into the soil at three different rubber contents (by weight) of 10%, 20% and 30%. The preliminary testing phase consisted of a series of consistency limits and free swell ratio tests, the results of which were analyzed to arrive at the optimum polymer concentration. The main test program included standard Proctor compaction, oedometer swell–compression, soil reactivity (shrink–swell index), cyclic wetting and drying, crack intensity, and micro–structure analysis by means of the scanning electron microscopy (SEM) technique. The improvement in swelling potential and swelling pressure was dependent on the rubber content, with polymer–treated mixtures holding a notable advantage over similar untreated cases. A similar dependency was also observed for the crack intensity factor and the shrink–swell index. The beneficial effects of rubber inclusion were compromised under the cyclic wetting and drying condition. However, this influence was eliminated where the rubber powder was paired with the polymer agent. A rubber inclusion of 20%, preferably paired with 0.2 g/l polymer, was suggested to effectively stabilize South Australian expansive soils.

**KEYWORDS**: Geosynthetics; Expansive soil; Rubber powder; Polymer; Swelling potential; Swelling pressure; Crack intensity; Cyclic wetting and drying.

Accepted manuscript doi:
10.1680/jgein.18.00009

## 1. Introduction

Previous testing conducted in South Australia indicates that the majority of soils in the state are expansive clays. The predominant soils are Hindmarsh and Keswick clays, which are abundantly found in high–population commercial and residential areas. Where exposed to seasonal environments, such soils are prone to significant volume changes, i.e. heave and settlements, thereby bringing forth instability concerns to the overlying structures. These concerns have incurred a large amount of maintenance costs, and thus demand engineering solutions to alleviate the associated socio–economic impacts on human's life. Chemical stabilization by means of traditional cementitious agents such as cement and lime is often implemented as a common soil improvement technique (e.g. Al-Rawas et al. 2005; Estabragh et al. 2014; Soltani et al. 2017[a]). Though effective, the application of such agents is often limited by leaching problems, and in some cases, may result in adverse effects when treating soils containing large amounts of organic matter, sulfates and salts (Sivapullaiah et al. 2000; Puppala et al. 2004; Hoyos et al. 2006). Other disadvantages include their inherent time–dependency nature, reduction in material workability, low durability against local environmental conditions (e.g. acidic and alkaline flows), high transportation costs, and rising environmental concerns due to greenhouse gas emissions (Rao et al. 2001; Guney et al. 2007; Estabragh et al. 2013; Georgees et al. 2015; Alazigha et al. 2016). As the global community is shifting towards a more sustainable mindset, alternate stabilization techniques capable of replacing or minimizing the need for such traditional agents have been highly encouraged. Beneficial reuse of solid waste materials and industrial by–products, e.g. carpet waste fibers, kiln dusts, silicate/calcium chloride geopolymers and demolition wastes, can be regarded amongst the most well–received propositions in this context (e.g. Mirzababaei et al. 2013[a], 2013[b]; Arulrajah et al. 2017[a], 2017[b], 2017[c]; Kua et al. 2017; Mirzababaei et al. 2017[a], 2017[b]; Suksiripattanapong et al. 2017; Phummiphan et al. 2018).

In Australia, it is estimated that 48 million tires are disposed each year, meaning that there is a relative abundance of waste tires available for recycling and beneficial reuse (Hannam 2014). Similar to fiber–reinforced soils, the rubber assemblage randomly distributes in the soil regime, and where optimized in dosage and geometry, amends the expansive soil with respect to moisture insensitivity (i.e. swell–shrink related volume changes), strength increase, and ductility improvement (e.g. Cetin et al. 2006; Akbulut et al. 2007; Özkul and Baykal 2007; Seda et al. 2007; Patil et al. 2011; Trouzine et al. 2012; Kalkan 2013; Srivastava et al.

Accepted manuscript doi:
10.1680/jgein.18.00009

2014; Signes et al. 2016; Yadav and Tiwari 2017[a]). A literature survey indicates a rather common emphasis on the application of coarse–graded tire rubber material, e.g. long tire rubber fibers. Such materials, however, would be associated with implementation difficulties when dealing with cohesive soils. On this basis, less regarded types of recycled tires such as tire rubber powder take the advantage of better workability, and thus add value if introduced to treat expansive soils.

Simple application procedures coupled with improved sustainability have promoted polymer–based additives as an attractive alternative to traditional cementitious agents. While commercially branded and readily accessible, such products have not yet received widespread acceptance among practicing engineers. This may be attributed to the lack of sufficient published data by independent establishments, and inadequate information provided by manufacturers regarding effective application rates or implementation procedures. A number of documented studies can be found which have assessed the efficiency of various polymer–based additives in treating expansive soils, thus mitigating the effect of swell–shrink related subsidence (e.g. Rauch et al. 2002; Inyang et al. 2007; Mirzababaei et al. 2009; Yazdandoust and Yasrobi 2010; Onyejekwe and Ghataora 2015; Alazigha et al. 2016; Ayeldeen and Kitazume 2017; Soltani et al. 2017[b]). Though promising, the reported results are not consistent on defining an ad hoc stabilization solution, and thus demands further examination.

The key to finding effective solutions to enhance the applications of expansive soils is to fundamentally understand their behavior in the face of changing moisture and temperature environments. For arid and semi–arid environments such as the Adelaide region of South Australia, this aspect is translated into alternate wetting and drying, incurred by changing periods of rainfall and drought. As such, prior promoting any stabilization technique as an effective scheme, its efficiency where exposed to periodic wetting and drying should be examined. A number of studies have assessed the volume change behavior of expansive soils treated with cementitious admixtures (e.g. Rao et al. 2001; Guney et al. 2007; Kalkan 2011; Estabragh et al. 2013) and polymer–based additives (e.g. Yazdandoust and Yasrobi 2010; Alazigha et al. 2016; De Camillis et al. 2017; Soltani et al. 2017[b]) during wetting and drying. However, the volume change behavior of expansive soil–rubber composites treated with polymer–based additives during wetting and drying has not yet been addressed in the literature.

Accepted manuscript doi:
10.1680/jgein.18.00009

The present study intends to examine the combined capacity of rubber powder inclusion and polymer–treatment in ameliorating the inferior engineering characteristics of a highly expansive soil found in Adelaide, South Australia. The experimental program was carried out in two phases consisting of preliminary and main tests. The preliminary testing phase consisted of a series of consistency limits and free swell ratio tests. The main test program included standard Proctor compaction, oedometer swell–compression, soil reactivity (shrink–swell index), cyclic wetting and drying, desiccation–induced cracking, and micro–structure analysis by means of the scanning electron microscopy (SEM) technique.

## 2. Materials

### 2.1. Soil

A large quantity of expansive clay was sourced from a landfill site in Adelaide, South Australia and was used for this study. This soil was characterized as *clay with high plasticity* (CH) in accordance with the Unified Soil Classification System (USCS). Mechanical properties of the soil, determined as per relevant ASTM and Australian standards, are summarized in **Table 1**. The grain–size distribution curve, as illustrated in **Figure 1**, indicated a clay fraction (<2 μm) of 44%, along with 36% silt (2–75 μm), 15% fine sand (0.075–0.425 mm), 4% medium sand (0.425–2 mm) and 1% coarse sand (2–4.75 mm). The swelling potential and free swell ratio (FSR) were, respectively, measured as 10.68% and 2.27, from which the soil was graded into *highly expansive* with respect to the classification criteria suggested by Seed et al. (1962) and Sridharan and Prakash (2000).

### 2.2. Tire Rubber Powder

Commercially available recycled tire rubber powder, supplied by a local distributor, was used to stabilize the expansive soil. **Figure 1** illustrates the grain–size distribution curve for the rubber particles, along with the used soil, determined as per the ASTM D422 standard. The rubber particles are similar in size to fine–medium sand, with particles ranging between 1.18 mm and 75 μm. The particle diameters corresponding to 10%, 30%, 50%, 60% and 90% finer (or passing) were measured as $d_{10}$=0.182 mm, $d_{30}$=0.334 mm, $d_{50}$=0.478 mm, $d_{60}$=0.513 mm and $d_{90}$=0.864 mm (see **Figure 1**). In addition, the uniformity (i.e. $C_u=d_{60}/d_{10}$) and curvature (i.e. $C_c=d_{30}^2/d_{10}d_{60}$) coefficients were determined as $C_u$=2.81 and $C_c$=1.20, from which the rubber particles were classified as *poorly–graded* in accordance with the USCS

Accepted manuscript doi:
10.1680/jgein.18.00009

criterion. **Figure 2** illustrates microscopic micrographs of the rubber particles at different magnification ratios. The rubber particles are non–spherical and irregular in shape (see **Figure 2b** at 50× magnification), with some cavities and micro–cracks propagated along the rubber's surface (see **Figure 2c** at 100× magnification), thus making for a rough surface texture. Such surface characteristics could potentially promote adhesion and/or induce interfacial friction between the rubber particles and the soil grains, thereby altering the soil fabric into a coherent matrix of restricted heave/settlement. Physical properties and chemical composition of the rubber particles, as supplied by the manufacturer, are provided in **Table 2**. The specific gravity (at 20$^{o}$C) was found to be 1.09, which is in compliance with that reported in the literature (see Yadav and Tiwari (2017$^{b}$) for details).

### 2.3. Polymer

A commercially manufactured polymer agent, hereafter referred to as PC, was used as the binder. PC, chemically referred to as polyacrylamide or PAM (–$CH_2CHCONH_2$–), is a water–soluble anionic synthetic polymer formed from acrylamide subunits. The anionic polymerization is accomplished through substituting $NH_2^-$ (amidogen) by $OH^-$ (hydroxide) (Seybold 1994). PAM is often employed to increase the viscosity of water or to encourage flocculation of clay particles present in water (Seybold 1994; Lu et al. 2002; Graber et al. 2006). PC, in particular, has been successfully implemented in Australian roadway construction as a suitable binder for a variety of clays, shales and gravels (Andrews and Sharp 2010; Camarena 2013; Georgees et al. 2015). It is supplied in granular form, and often diluted with water (i.e. 200 g of PC into 1000 l of water, as recommended by the manufacturer) for application. Other properties include a specific gravity (at 25°C) of 0.8 and a pH (at 25°C) of 6.9.

## 3. Experimental Work

The rubber powder was incorporated into the soil at three different rubber contents (defined as rubber to dry soil weight ratio), i.e. $R_c$=10%, 20% and 30%. The experimental program was carried out in two phases consisting of preliminary and main tests. The preliminary testing phase included a series of consistency limits and free swell ratio tests. The intention of the preliminary testing phase was to identify a PC concentration rate capable of yielding an effective soil–rubber stabilization scheme. The natural soil and various soil–rubber mixtures were examined with three different PC concentrations (defined as weight of

Accepted manuscript doi:
10.1680/jgein.18.00009

PC to volume of water ratio), i.e. 0.2 g/l (manufacturer–recommended), 0.4 g/l and 0.6 g/l. The consistency limits, i.e. liquid limit, plastic limit, plasticity index and linear shrinkage, were measured as per Australian standards (see relevant standard designations in **Table 1**). The free swell ratio is defined as the ratio of equilibrium sediment volume of 10 g oven–dried soil passing sieve 425 μm in water (or in the case of this study PC solution) to that of kerosene (Sridharan and Prakash 2000). As a consequence of rubber particles floating on water, only the natural soil was tested for the free swell ratio. Hereafter, the following coding system is adopted to designate the various mix designs:

$$NR_xP_y \quad (1)$$

where N=natural soil; $R_x$=x% rubber (x=0, 10%, 20% and 30%); and $P_y$=y g/l PC (y=0, 0.2 g/l, 0.4 g/l and 0.6 g/l). The natural with no additives is, therefore, denoted as $NR_0P_0$. As a typical example, $NR_{20}P_{0.4}$ represents the natural soil mixed with 20% rubber and treated with 0.4 g/l PC. A total of 16 mix designs were tested for consistency limits during the preliminary testing phase, whereas only four scenarios, i.e. $NR_0P_0$, $NR_0P_{0.2}$, $NR_0P_{0.4}$ and $NR_0P_{0.6}$., were considered for the free swell ratio test.

The main test program was carried out on the natural soil and various soil–rubber mixtures without and with the optimum PC concentration. Hereafter, the former will be referred to as untreated, while the latter will be denoted as treated. The optimum PC concertation was selected as 0.2 g/l based on the preliminary test results, which will be further discussed in **Section 4.1**. The main test program consisted of the following tests: **i)** standard Proctor compaction; **ii)** oedometer swell–compression; **iii)** soil reactivity (shrink–swell index); **iv)** cyclic wetting and drying; **v)** desiccation–induced cracking; and **vi)** micro–structure (SEM) analysis. The methodology associated with each component of the main test program will be further outlined in detail.

### 3.1. Compaction Studies and Sample Preparation

A series of standard Proctor compaction tests were carried out on the natural soil ($NR_0P_0$) and various soil–rubber mixtures, untreated and treated with 0.2 g/l PC, in accordance with the ASTM D698 standard. Samples for the oedometer swell–compression, soil reactivity (shrink–swell index), cyclic wetting and drying and SEM tests were prepared by the static compaction technique at the corresponding optimum moisture content and maximum dry unit weight of each mixture (see **Table 3**). The required amount of water or PC solution (with 0.2

Accepted manuscript doi:
10.1680/jgein.18.00009

g/l concentration) corresponding to the desired optimum moisture content was added to each mixture, and thoroughly mixed by hand. Extensive care was dedicated to pulverize the lumped particles, targeting homogeneity of the mixtures. Mixtures were then enclosed in plastic bags and stored under room temperature conditions for 24 hours, ensuring even distribution of moisture throughout the soil mass. A special split mold, similar to that described in Soltani et al. (2017[a]), was designed and fabricated from stainless steel to accomplish static compaction. The mold consisted of three sections, i.e. the top collar, the middle oedometer ring, and the bottom collar. The oedometer ring measures 50 mm in diameter and 20 mm in height, and accommodates the sample for oedometer testing conditions. The moist mixtures were compressed in the mold at three layers by a constant displacement rate of 1.5 mm/min to a specific compaction load, each layer having attained the desired/target maximum dry unit weight. The surface of the first and second compacted layers were scarified to ensure a good bond between adjacent layers of the mixture. Samples for the simplified core shrinkage test (i.e. a component of the soil reactivity test, as further outlined in **Section 3.3**) were prepared in a similar fashion. In this case, however, a different mold with a middle section measuring 50 mm in diameter and 100 mm in height, along with five compaction layers, was adopted. As a consequence of rubber particles floating on water, standard procedures outlined in the ASTM D854 (2014) standard for measuring the specific gravity of particles were not applicable. Therefore, the average specific gravity of various soil–rubber mixtures was estimated by the following theoretical equation (Trouzine et al. 2012):

$$G_{sm} = \frac{G_{ss} G_{sr} (w_s + w_r)}{w_s G_{sr} + w_r G_{ss}} \tag{2}$$

where $G_{sm}$=specific gravity of soil–rubber mixture; $w_{ss}$=weight of dry soil; $w_r$=weight of rubber particles; $G_{ss}$=specific gravity of soil solids (=2.67); and $G_{sr}$=specific gravity of rubber particles (=1.09).

Basic mechanical properties of the prepared samples used for the main tests are summarized in **Table 3**. A total of eight mix designs, divided into two groups of untreated (designated as $NR_0P_0$, $NR_{10}P_0$, $NR_{20}P_0$ and $NR_{30}P_0$) and treated with 0.2 g/l PC (designated as $NR_0P_{0.2}$, $NR_{10}P_{0.2}$, $NR_{20}P_{0.2}$ and $NR_{30}P_{0.2}$), were considered for the main experimental program.

Accepted manuscript doi:
10.1680/jgein.18.00009

### 3.2. Oedometer Swell–Compression Test

The prepared samples were subjected to a series of oedometer swell–compression tests as specified in the ASTM D4546 (2014) standard. The test included two stages, i.e. swell and compression. In the first stage, the desired sample was allowed to freely swell under a low nominal overburden stress of $\sigma'_0$=7 kPa. The incurred axial swelling strain or heave was recorded during various time intervals to a point in which swell–time equilibrium, a state corresponding to the sample's swelling potential (defined as the ultimate axial swelling strain), was achieved. During the compression stage, the swollen sample was gradually loaded to counteract the built–up axial swelling strain. The stress required to retain the sample's initial placement condition (or void ratio $e_0$, as outlined in **Table 3**) was taken as the swelling pressure (Sridharan et al. 1986).

The conventional oedometer swell test has been regarded as the most common technique to assess the soil's expansive potential or degree of expansivity (Sridharan and Keshavamurthy 2016). Some limitations, however, include its dependency to the sample's initial moisture condition and not accounting for suction variations. Some of the more common classification procedures for expansive soils, developed with respect to percent expansion in oedometer under $\sigma'_0$=7 kPa (Holtz and Gibbs 1956; Seed et al. 1962; Sridharan and Prakash 2000), are summarized in **Table 5**.

### 3.3. Soil Reactivity Test and the Shrink–Swell Index

The shrink–swell index, determined in accordance with the AS 1289.7.1.1 (2003) standard, can be characterized as a direct method of evaluating the soil's degree of expansivity (referred to as reactivity in Australian geotechnical practice). Other significant applications include its widespread use for predicting free surface ground movements (Cameron 1989; Fityus et al. 2005). Despite its successful adoption in routine geotechnical practice in Australia, its existence and use within Australia have not been widely recognized by the international geotechnical community (Fityus et al. 2005). The shrink–swell index requires incorporating test results obtained from the simplified core shrinkage and the modified oedometer swell tests, which are further presented in detail:

- In the simplified core shrinkage test, the desired cylindrical sample, measuring 50 mm in diameter and 100 mm in height (see **Section 3.1**), is allowed to desiccate under room temperature conditions. The variations of axial shrinkage strain is monitored during

Accepted manuscript doi:
10.1680/jgein.18.00009

various time intervals to a point in which shrinkage ceases. The sample is then oven–dried at 105°C to remove any remaining moisture. Final height measurements are taken by a Vernier caliper, from which the sample's ultimate shrinkage strain, denoted as $\varepsilon_{sh}$, can be derived.

- The modified oedometer swell test is essentially similar to the first stage of the oedometer swell–compression test, as outlined in **Section 3.2**. In this case, however, a higher nominal overburden stress equal to $\sigma'_0$=25 kPa is adopted. The ultimate axial swelling strain upon achieving swell–time equilibrium is denoted as $\varepsilon_{sw}$.

Finally, the shrink–swell index $I_{ss}$ is obtained by the following (AS 1289.7.1.1 2003):

$$I_{ss} = \frac{\varepsilon_{sh} + \frac{1}{2}\varepsilon_{sw}}{1.8} \quad (3)$$

The denominator in **Equation 3** is an empirical coefficient, which is defined as the range of total suction change with respect to the soil's volume increase from air–dry to near saturation condition. The range of total suction change is commonly taken as 1.8 pF (pF=potential of free energy, which is a unit for soil suction and is related to kilopascals through pF=1+log[kPa]) for the majority of reactive soils in Australia. This value was suggested based on collective experience of the AS 2870 (2011) code committee, and is supported by the observation that the majority of volume change takes place in a linear manner between the wilting point for trees and a moisture content close to saturation (Fityus et al. 2005). Previous studies have reported the wilting point suction to vary between 4.0 pF and 4.4 pF (Wray 1998; Cameron 2001). Furthermore, the variations of total suction at moisture contents near saturation state have been reported to fall in the range of 2.2 pF to 2.5 pF (Fityus et al. 2005). As such, the suggested value of 1.8 pF can be deemed as reasonable. The shrink–swell index represents percentage axial strain, either swelling or shrinkage, per change in unit suction of the soil (i.e. $\%pF^{-1}$). Thus, it is expected to address some limitations associated with other expansive soil classification criteria which are either dependent on the soil's initial moisture condition or do not account for suction variations (e.g. the conventional oedometer swell test, as outlined in **Table 5**). Classification procedures for expansive soils with respect to the shrink–swell index, as suggested by Seddon (1992), are summarized in **Table 6**.

### 3.4. Cyclic Wetting and Drying Test

Accepted manuscript doi:
10.1680/jgein.18.00009

Similar to the first step in the oedometer swell–compression test (see **Section 3.2**), the desired sample was allowed to freely swell under $\sigma'_0$=7 kPa resulting from a cylindrical load directly applied to the sample. Upon completion of the wetting process (i.e. achieving swell–time equilibrium), reservoir water was drained through a drainage valve embedded within the oedometer cell. The oedometer cell, along with the cylindrical load, were then transferred to an oven set to a constant temperature of 40$^{o}$C for drying. The drying process was carried out for about five days to ensure shrinkage equalization. The combination of one wetting and the subsequent drying stage is designated as one wetting–drying cycle. Alternate wetting and drying of the sample was repeated in a similar fashion to a point in which the swelling potential subject to two successive cycles reached a nearly constant value. In this study, four mix designs, i.e. $NR_0P_0$, $NR_{30}P_0$, $NR_0P_{0.2}$ and $NR_{30}P_{0.2}$, were tested for cyclic wetting and drying.

The swelling potential may either decrease or increase with increase in number of applied wetting–drying cycles, and regardless of the observed trend, further converges to a nearly constant value upon the completion of several cycles (Soltani et al. 2017[b]). This state is defined as swell–shrink (or elastic) equilibrium, which signifies a transitional deformation state where the plastic (or irreversible) deformation incurred in the soil structure (during wetting and drying) largely fades out, and thus change to elastic (or reversible) in character (Tripathy et al. 2002; Alonso et al. 2005; Estabragh et al. 2015). In this study, the equilibrium condition was achieved at the fourth cycle, thus only five cycles were implemented for the tested samples.

### 3.5. Desiccation–Induced Crack Studies

Desiccation–induced cracking can adversely influence the performance of various soil structures (e.g. excavations, earth slopes, highway embankments and clay liners), and thus assumes a significant role in fulfilling design criteria when constructing on expansive soils. The intensity of cracks is commonly quantified by means of the crack intensity factor (CIF) and the crack reduction factor (CRF), which are defined as (Yesiller et al. 2000; Miller and Rifai 2004):

$$\mathrm{CIF} = \frac{A_c}{A_0} \times 100 \tag{4}$$

$$CRF = \frac{CIF_n - CIF_s}{CIF_n} \quad (5)$$

where $A_c$=area of cracks; $A_0$=initial area of the tested sample; $CIF_n$=crack intensity factor for the natural soil ($NR_0P_0$); and $CIF_s$=crack intensity factor for the stabilized sample.

Desiccation–induced crack tests were carried out on the natural soil and various soil–rubber mixtures (untreated and treated with 0.2 g/l PC) prepared by the slurry technique at their respective liquid limit, as commonly adopted in the literature (e.g. Tang et al. 2012; Costa et al. 2013; Chaduvula et al. 2017). The required amount of water or PC solution corresponding to the desired liquid limit (see **Table 3**) was added to each mixture, and thoroughly mixed to obtain slurries of uniform consistency. The resultant slurries were poured into petri dishes, measuring 100 mm in diameter and 15 mm in height, and gently tapped on a wooden platform to remove entrapped air. To simulate severe ambient conditions of the Adelaide region, samples were allowed to desiccate under a constant temperature of 40$^o$C. Upon the completion of drying (moisture equalization), still photographs were taken using a high resolution digital camera fixed at a vertical angle 50 cm above the desiccated samples. The ImageJ software package was then implemented to quantify the crack features.

### 3.6. Scanning Electron Microscopy (SEM)

Significant information on the micro–structure can be obtained by the scanning electron microscopy (SEM) technique. Typical mixtures including $NR_0P_0$, $NR_{20}P_0$, $NR_0P_{0.2}$ and $NR_{20}P_{0.2}$ were investigated. The desired samples, prepared as per **Section 3.1**, were allowed to air–dry for about 14 days. The samples were then carefully fractured into small cubic–shaped pieces corresponding to a volume of approximately 1 cm$^3$, as suggested in the literature (e.g. Tang et al. 2007; Mirzababaei et al. 2009; Yazdandoust and Yasrobi 2010), and further scanned over various magnification ratios ranging from 250× to 20,000×. In this study, the Philips XL20 SEM device, with a resolution of 4 μm and a maximum magnification ratio of 50,000×, was used for scanning electron microscopy imaging.

## 4. Results and Discussion

### 4.1. Consistency Limits and the Free Swell Ratio

**Figures 3a**, **3b** and **3c** illustrate the variations of liquid limit *LL*, plasticity index *PI* and linear shrinkage *LS* against PC concentration for the tested mix designs (i.e. $NR_xP_y$; where

Accepted manuscript doi:
10.1680/jgein.18.00009

x=0, 10%, 20% and 30%, and y=0, 0.2 g/l, 0.4 g/l and 0.6 g/l), respectively. Untreated soil–rubber mixtures ($NR_xP_0$) exhibited lower consistency limits compared with that of the natural soil ($NR_0P_0$). In this case, the higher the rubber content the lower the consistency limits, following a monotonic decreasing trend. For instance, the natural soil resulted in *LL*=78.04%, while the inclusion of 10%, 20% and 30% rubber resulted in *LL*=73.32%, 68.59% and 65.58%, respectively. It is well–accepted that the consistency limits are primarily a function of the mixture's clay content. An increase in rubber content substitutes a larger portion of the clay content, and thus leads to lower consistency limits. The lower specific surface area and water adsorption capacity of the rubber particles compared with the soil grains also contributes to lower consistency limits (Cetin et al. 2006; Trouzine et al. 2012; Srivastava et al. 2014). As a result of PC–treatment, the natural soil experienced a notable increase in the consistency limits. The magnitude of increase, however, was observed to be independent from the adopted PC concertation, as all three concentrations exhibited similar results with marginal differences (see $NR_0P_y$ in **Figure 3**). As a typical case, *LL* increased from 78.04% for the natural soil ($NR_0P_0$) to 87.61%, 87.22% and 85.80% for $NR_0P_{0.2}$, $NR_0P_{0.4}$ and $NR_0P_{0.6}$, respectively. An increase in the consistency limits, the liquid limit in particular, implies that a flocculated fabric dominates the clay–rubber matrix (Mitchell and Soga 2005). As opposed to a face–to–face aggregated (or dispersed) fabric, an edge–to–face flocculated fabric offers more resistance to shear (or cone penetration), thereby leading to an increased liquid limit. PAM molecules are hydrophilic in nature, and thus provide additional adsorption sites for water molecules, which in turn contributes to higher consistency limits (Kim and Palomino 2009).

The location of the tested mix designs on Cassgrande's plasticity chart is illustrated in **Figure 4**. All mixtures lie within the CH region (*clay with high plasticity*) of the plasticity chart. The variations of *PI* against *LL* followed a linear path nearly parallel to the A–line of the plasticity chart, i.e. *PI*=0.73(*LL*–20). In this case, a conventional regression analysis indicated the existence of a strong linear agreement in the form of *PI*=0.77(*LL*–6.84) (with $R^2$=0.989) for the tested mixtures. For a given PC concentration, an increase in rubber content relocated the soil towards lower plasticity regions (e.g. see the typical linear trendline for $NR_xP_0$ in **Figure 4**). On the contrary, for a given soil–rubber mixture (constant rubber content), PC–treatment repositioned the soil towards higher plasticity regions (e.g. see the typical arrowed path linking $NR_0P_0$ to $NR_0P_y$ in **Figure 4**). The magnitude of increase in *LL*

Accepted manuscript doi:
10.1680/jgein.18.00009

and *PI*, however, was observed to be independent from the adopted PC concentration, as evident with the clustering of data points at constant rubber contents (compare $NR_xP_{0.2}$ with $NR_xP_{0.4}$ and $NR_xP_{0.6}$ in **Figure 4** at any arbitrary x value).

Results of the free swell ratio tests are summarized in **Table 4**. Suspension of the soil in distilled water ($NR_0P_0$) resulted in a free swell ratio of FSR=2.27. Where suspended in PC solutions of 0.2 g/l, 0.4 g/l and 0.6 g/l, FSR was measured as 1.67, 1.63 and 1.53, respectively. Classification procedures for expansive soils with respect to the FSR value, as suggested by Sridharan and Prakash (2000), are outlined in **Table 4**. The natural soil was classified as *highly expansive*, while PC–treated mixtures ($NR_0P_{0.2}$, $NR_0P_{0.4}$ and $NR_0P_{0.6}$) manifested a *moderate* degree of expansivity. As evident with the FSR values and their corresponding classifications, excessive PC concentrations, i.e. 0.4 g/l and 0.6 g/l, seem not to provide additional improvements.

Basic geotechnical properties such as the consistency limits and the free swell ratio can be employed to infer the soil's fabric, and thus arrive at initial judgements on the performance of various polymer agents at different concentrations (Worth and Wood 1978; Prakash and Sridharan 2004; Mitchell and Soga 2005). Taking into account the discussed results, the three adopted PC concentrations were observed to yield similar results with marginal differences. Therefore, the manufacturer–recommended concentration of 0.2 g/l was deemed as satisfactory, and thus was used for the main tests the results of which will be further presented and discussed in detail.

### 4.2. Compaction Characteristics

Standard Proctor compaction curves, along with corresponding zero air void (ZAV) saturation lines, for the natural soil ($NR_0P_0$) and various soil–rubber mixtures untreated and treated with 0.2 g/l PC are provided in **Figures 5a** and **5b**, respectively. As a result of rubber inclusion, the natural soil exhibited a notable reduction in both the maximum dry unit weight $\gamma_{dmax}$ and the optimum moisture content $\omega_{opt}$ (see the trendline in **Figure 5a**). As a result of PC–treatment, a marginal increase in both $\gamma_{dmax}$ and $\omega_{opt}$ was noted for the natural soil (compare $NR_0P_0$ with $NR_0P_{0.2}$ in **Figure 5b**), while treated soil–rubber mixtures exhibited a trend similar to that observed for similar untreated cases (see the trendline in **Figure 5b**). Decrease in $\gamma_{dmax}$ and $\omega_{opt}$ as a result of the rubber inclusions can be attributed to the lower specific gravity, specific surface area and water adsorption capacity of the rubber particles

Accepted manuscript doi:
10.1680/jgein.18.00009

compared with the soil grains (Akbulut et al. 2007; Özkul and Baykal 2007; Seda et al. 2007; Kalkan 2013; Signes et al. 2016).

### 4.3. Swelling Characteristics

4.3.1. Swelling Potential and Swelling Pressure

Swell–time curves, represented by the two–parameter rectangular hyperbola function (e.g. Sivapullaiah et al. 1996; Sridharan and Gurtug 2004; Soltani et al. 2017[a]), for the natural soil ($NR_0P_0$) and various soil–rubber composites untreated and treated with 0.2 g/l PC are provided in **Figures 6a** and **6b**, respectively. As a result of rubber inclusion and/or PC–treatment, the swell–time locus experienced a major downward shift over the $\varepsilon_a$:log$t$ space ($\varepsilon_a$=axial swelling strain; and $t$=time), indicating a significant reduction in the magnitude of exhibited swelling strain, and thus swelling potential (defined as the ultimate axial swelling strain) compared with the natural soil. At $t$=24 hr, for instance, the natural soil resulted in a swelling strain of $\varepsilon_a(t)$=9.65%, while the inclusion of 10%, 20% and 30% rubber resulted in $\varepsilon_a(t)$=7.55%, 6.35% and 4.85%, respectively (see **Figure 6a**). Similar treated samples exhibited a more pronounced decreasing trend, where the above given values dropped to $\varepsilon_a(t)$=6.45% ($NR_0P_{0.2}$), 5.25%, 3.25% and 2.43%, respectively (see **Figure 6b**). The natural soil and soil–rubber mixtures corresponding to $R_c$=10%, 20% and 30% resulted in swelling potential values of $S_p$=10.68%, 8.48%, 7.26% and 5.73%, respectively. As a result of PC–treatment, however, the aforementioned values further decreased to $S_p$=7.15%, 6.20%, 4.28% and 3.20%, respectively.

**Figure 7** illustrates the variations of swelling pressure and swelling potential against rubber content for the tested samples. The variations of swelling pressure $P_s$ followed a trend similar to that observed for swelling potential $S_p$, and indicated that, the higher the rubber content the greater the reduction in $S_p$ and $P_s$, with treated samples holding a notable advantage over similar untreated cases (compare $NR_xP_0$ with $NR_xP_{0.2}$ in **Figure 7**). The natural soil ($NR_0P_0$) and soil–rubber mixtures corresponding to $R_c$=10%, 20% and 30% resulted in $P_s$=235 kPa, 131 kPa, 124 kPa and 93 kPa, respectively. Where treated with 0.2 g/l PC, these values dropped to $P_s$=165 kPa ($NR_0P_{0.2}$), 107 kPa, 86 kPa and 35 kPa, respectively. The classification criterion proposed by Seed et al. (1962) (see **Table 5**) was implemented to assess the expansive potential of the tested samples, and the results are depicted in **Figure 7**. The two mix designs containing 30% rubber inclusion ($NR_{30}P_0$ and

$NR_{30}P_{0.2}$) were classified as *moderately expansive* (specified as 'M'), while other samples were graded into *highly expansive* (specified as 'H').

As demonstrated in **Figure 8**, the evolution of swelling with time, represented by an *S*–shaped curve over the $\varepsilon_a$:log*t* space, takes place at three stages, i.e. the initial, primary and secondary swelling (Sivapullaiah et al. 1996; Sridharan and Gurtug 2004; Rao et al. 2006; Soltani et al. 2017[b], 2018). The initial swelling phase, also recognized to as inter–void swelling, occurs at macro–structural level, and results in small volume changes mainly less than 10% of the total volume increase (<10%$S_p$). The primary swelling phase constitutes for up to 80% of the total volume increase (≈80%$S_p$), and is graphically represented by a steep–sloped linear portion bounded by the initial and primary swelling time margins. The secondary swelling phase takes place as a result of double–layer repulsion, and accounts for small time–dependent volume changes. As opposed to the initial swelling phase, both the primary and secondary swelling phases evolve at micro–structural level where swelling of active clay minerals takes place. Critical variables obtained from the *S*–shaped curve, defined as swell–time characteristics, can be adopted to describe the time–dependency nature of the swelling phenomenon. These variables, as outlined in **Figure 8**, are characterized as: **i)** completion time of the initial and primary swelling phases ($t_{is}$ and $t_{ps}$); **ii)** initial, primary and secondary swelling strains ($\varepsilon_{ais}$, $\varepsilon_{aps}$ and $\varepsilon_{ass}$; $S_p=\varepsilon_{ais}+\varepsilon_{aps}+\varepsilon_{ass}$); and **iii)** primary and secondary swelling rates ($C_{ps}$ and $C_{ss}$), which are defined as (Soltani et al. 2018):

$$C_{ps}=\frac{\Delta\varepsilon_a}{\Delta\log t}\Bigg]_{t=t_{is}}^{t=t_{ps}}=\frac{\varepsilon_{aps}}{\log\left(\frac{t_{ps}}{t_{is}}\right)} \tag{6}$$

$$C_{ss}=\frac{\Delta\varepsilon_a}{\Delta\log t}\Bigg]_{t=t_{ps}}^{t=t_{ss}}=\frac{\varepsilon_{ass}}{\log\left(\frac{t_{ss}}{t_{ps}}\right)} \tag{7}$$

where $t_{ss}$=completion time of the secondary swelling phase (=14,400 min).

Swell–time characteristics for the tested samples are summarized in **Table 7**. The primary and secondary swelling strains mainly demonstrated a trend similar to that observed for the swelling potential $S_p$, meaning that $R_c$=30% promoted the lowest $\varepsilon_{aps}$ and $\varepsilon_{ass}$ values for both untreated and treated soil–rubber mixtures (see $NR_{30}P_0$ and $NR_{30}P_{0.2}$ in **Table 7**). **Figures 9a** and **9b** illustrate the variations of $C_{ps}$ and $C_{ss}$ against rubber content for the tested samples, respectively. The rubber inclusions led to a noticeable reduction in both $C_{ps}$ and $C_{ss}$,

Accepted manuscript doi:
10.1680/jgein.18.00009

indicating a capacity of counteracting the heave in both magnitude and time. The higher the rubber content the lower the swelling rates, following a monotonic decreasing trend, with treated samples exhibiting more efficiency in reducing $C_{ps}$ and $C_{ss}$ compared with similar untreated cases (compare $NR_xP_0$ with $NR_xP_{0.2}$ in **Figure 9**). For the natural soil ($NR_0P_0$), $C_{ps}$ and $C_{ss}$ were measured as $4.85\times10^{-2}$ and $1.07\times10^{-2}$, respectively. As optimal cases, these values, respectively, dropped to $2.63\times10^{-2}$ and $7.06\times10^{-3}$ for $NR_{30}P_0$, and $1.50\times10^{-2}$ and $5.28\times10^{-3}$ for $NR_{30}P_{0.2}$.

4.3.2. Shrink–Swell Index

Variations of the shrinkage and swelling strains, i.e. $\varepsilon_{sh}$ and $\varepsilon_{sw}$, along with corresponding shrink–swell index values, are provided in **Figure 10**. Increase in rubber content led to a noticeable reduction in both $\varepsilon_{sh}$ and $\varepsilon_{sw}$, and thus the shrink–swell index $I_{ss}$. For the treated cases, however, a more pronounced decreasing trend can be observed (compare $NR_xP_0$ with $NR_xP_{0.2}$ in **Figure 10**). The degree of expansivity, in this case referred to as reactivity, was characterized in accordance with the Seddon (1992) classification criterion (see **Table 6**), and the results are depicted in **Figure 10**. The natural soil ($NR_0P_0$) was graded into *highly reactive* ($H^R$) corresponding to $I_{ss}$=4.21 $\%pF^{-1}$. For untreated cases, $R_c$=10%, 20% and 30% resulted in $I_{ss}$=3.30 $\%pF^{-1}$, 2.12 $\%pF^{-1}$ and 1.49 $\%pF^{-1}$, and thus classified as *moderately*/*highly reactive* ($M^R/H^R$), *moderately reactive* ($M^R$) and *slightly reactive* ($S^R$), respectively. Where treated with 0.2 g/l PC, the aforementioned values dropped to $I_{ss}$=2.51 $\%pF^{-1}$ ($M^R$), 1.88 $\%pF^{-1}$ ($M^R$), 1.80 $\%pF^{-1}$ ($M^R$) and 1.04 $\%pF^{-1}$ ($S^R$), respectively.

4.3.3. Amending Mechanisms

Similar to fiber–reinforced soils, the rubber inclusions are able to amend the soil fabric through improvements achieved in three aspects: **i)** increase in non–expansive fraction, which is a function of rubber content; **ii)** interlocking of rubber particles and soil grains; and **iii)** interfacial frictional resistance generated as a result of soil–rubber contact (Tang et al. 2007; Al-Akhras et al. 2008; Viswanadham et al. 2009[a], 2009[b]; Tang et al. 2010; Patil et al. 2011; Trouzine et al. 2012; Kalkan 2013; Estabragh et al. 2014; Phanikumar and Singla 2016; Soltani et al. 2018; Yadav and Tiwari 2017[a]). The randomly distributed rubber particles resemble a spatial three–dimensional network in favor of weaving (or interlocking) the soil grains into a coherent matrix of restricted heave. The greater the number of included rubber particles (i.e. increase in rubber content) the more effective the interlocking effect. Frictional

Accepted manuscript doi:
10.1680/jgein.18.00009

resistance grows as a consequence of rubber particles experiencing tensile stress in the presence of strong swelling forces. This interfacial resistance is a function of soil–rubber contact area, with greater contact levels offering a higher resistance to swelling. Consequently, this amending mechanism is in line with rubber content. The greater the number of included rubber particles the greater the soil–rubber contact level, which in turn promotes an induced interfacial frictional resistance capable of counteracting swelling with more efficiency.

The type of polymer charge, i.e. cationic, non–ionic or anionic, strongly influences the degree of polymer adsorption/attraction to clay particles. Positively charged polymers are electrostatically attracted to the negatively charged clay surface, while non–ionic polymers accomplish adsorption through van der Waals and/or hydrogen bonding (Theng 1982; Wallace et al. 1986; Miller et al. 1998). Even though anionic polymers, such as the one used in this study, tend to be repelled by clay particles (owing to charge repulsion), adsorption can still take place through the presence of cations acting as bridges. The degree of attraction in this case is dependent on the amount and type of exchangeable cations, clay content, pH and polymer molecular size (Theng 1982; Lu et al. 2002; Rabiee et al. 2013). Polyvalent cations such as $Ca^{2+}$ and $Mg^{2+}$, for instance, offer greater efficiency in attracting the carboxylate groups on the polymer chains compared with univalent cations such as $Na^{+}$ (Letey 1994; Laird 1997). As such, the role of PC in controlling the effect of swelling can be attributed to its ability to form ionic bonds holding clay particles together through the cationic bridging mechanism, thereby shrinking the electrical double layer. This in turn induces flocculation of clay particles by forming coarse aggregates, which is further accompanied by a reduction in the clay content size, and thus a reduction in the swelling behavior. Where paired with rubber, PC–treatment may further enhance the interlocking of rubber particles and soil grains, thus promoting a greater reduction in swelling compared with similar untreated cases.

4.3.4. Cyclic Wetting and Drying

**Figure 11** illustrates the variations of swelling potential $S_p$ against number of applied wetting–drying cycles $n$ for the samples $NR_0P_0$, $NR_{30}P_0$, $NR_0P_{0.2}$ and $NR_{30}P_{0.2}$. With regard to untreated cases ($NR_0P_0$ and $NR_{30}P_0$), $S_p$ exhibited a rise–fall behavior, peaking at the second cycle and then decreasing to an equilibrium value upon the completion of five cycles. The treated samples ($NR_0P_{0.2}$ and $NR_{30}P_{0.2}$), however, demonstrated a monotonic decreasing trend

Accepted manuscript doi:
10.1680/jgein.18.00009

with lower $S_p$ values compared with similar untreated cases. At the first cycle ($n$=1), the samples were allowed to swell from their respective optimum moisture content, thus the Seed et al. (1962) classification criterion, which complies with the initial placement condition (see **Table 5**), was implemented to assess the expansive potential of the tested samples. With regard to other cycles ($n$≥2), where the samples undergo swelling from an initially dry condition (due to the previous drying cycle), the two classification criteria suggested by Holtz and Gibbs (1956) and Sridharan and Prakash (2000) (see **Table 5**) were adopted. The classification results are summarized in **Table 8**. The classifications were either maintained or improved as a result of rubber inclusion and/or PC–treatment, thus indicating that the beneficial effects of both stabilization agents in counteracting the swell–shrink related volume changes were fairly preserved under the influence of alternate wetting and drying. Upon the completion of five cycles, a slight increase in $S_p$ was noted for the untreated sample containing 30% rubber inclusion (see $NR_{30}P_0$ in **Figure 11**), i.e. $S_p(1)$=5.73% against $S_p(5)$=6.20%. This implies that the blending of rubber particles and soil grains, obtained by compaction, could potentially be compromised under the influence of alternate wetting and drying. As a result of PC–treatment, however, the interlocking of rubber particles and soil grains, enhanced by the polymer binder, remains intact during successive cycles (compare $NR_{30}P_0$ with $NR_{30}P_{0.2}$ in **Figure 11**).

Reduction in swelling potential as a result of alternate wetting and drying can be attributed to the reconstruction of the clay micro–structure upon completion of the first or second cycle (Dif and Bluemel 1991; Zhang et al. 2006; Kalkan 2011; Estabragh et al. 2015). Capillary stresses generated as a consequence of drying facilitate the formation of strong van der Waals bonds, promoting cementation and aggregation of clay particles. This is followed by the development of some relatively large inter–pores among the aggregated soil lumps, which decreases the available surface for interaction with water, thereby reducing the specific surface area and plasticity of the clay content accompanied by a decreased tendency for swelling (Basma et al. 1996; Zhang et al. 2006; Estabragh et al. 2013; Soltani et al. 2017[b]).

### 4.4. Crack Intensity

Variations of the crack intensity factor (CIF), along with corresponding crack reduction factors (CRF), are provided in **Figure 12**. In addition, crack patterns observed for the tested samples are illustrated in **Figure 13**. The rubber inclusions were able to amend desiccation–

Accepted manuscript doi:
10.1680/jgein.18.00009

induced cracking. In this case, the higher the rubber content the greater the improvement, with PC–treated mixtures holding a notable advantage over similar untreated cases (compare $NR_xP_0$ with $NR_xP_{0.2}$ in **Figure 12**). A typical hierarchical cracking pattern can be observed for the natural soil, which divides the soil mass into a series of rather small cells with wide crack openings. On the contrary, soil–rubber mixtures manifested larger cells with relatively smaller crack openings (e.g. compare $NR_0P_0$ with $NR_{20}P_0$ and $NR_{20}P_{0.2}$). The natural soil ($NR_0P_0$) and soil–rubber mixtures corresponding to $R_c$=10%, 20% and 30% resulted in CIF=23.67%, 16.79%, 9.03% and 4.73% (i.e. CRF=29.06%, 61.86% and 80.01%), respectively. Similar mixtures treated with 0.2 g/l PC resulted in lower CIF and higher CRF values. In this case, the aforementioned values dropped to CIF=15.57%, 11.90%, 7.74% and 2.47% (i.e. CRF=34.21%, 49.73%, 67.32% and 89.56%), respectively.

As a consequence of internal restrains (e.g. non–uniform drying) and/or external restrains (e.g. boundary friction/adhesion) acting on the soil during drying, tensile stresses developed within the soil can exceed the soil's tensile strength, thus resulting in the development and propagation of cracks (Konrad and Ayad 1997; Kodikara and Chakrabarti 2005; Nahlawi and Kodikara 2006; Tang et al. 2012; Costa et al. 2013). The development and propagation of cracks are primarily a function of clay content, meaning that the higher the clay content the greater the intensity of cracks (Mitchell and Soga 2005). As such, the rubber inclusions are able to amend the soil fabric through clay–substitution. Consequently, this amending mechanism is a function of rubber content, with higher rubber inclusions substituting a larger portion of the clay content, and thus ameliorating the effect of cracking with increased efficiency. The ductile character of the rubber particles can complement a notable improvement in the soil's tensile strength, thus restricting the propagation of cracks. Increase in the soil's tensile strength may also be achieved through interlocking of rubber particles and soil grains. As previously discussed (see **Section 4.3.3**), the interlocking effect can be considered as a direct function of rubber content, and it is further enhanced in the presence of the polymer binder.

### 4.5. Micro–Structure (SEM) Analysis

**Figures 14a**–**14d** illustrate SEM micrographs for the samples $NR_0P_0$, $NR_{20}P_0$, $NR_0P_{0.2}$ and $NR_{20}P_{0.2}$, respectively. The micro–fabric of the natural soil ($NR_0P_0$) included a number of large inter– and intra–assemblage pore–spaces formed between and within the clay

Accepted manuscript doi:
10.1680/jgein.18.00009

aggregates, respectively (see **Figure 14a**). The inter–assemblage pore–spaces are formed during sample preparation (or compaction), and thus are directly proportional to the sample's initial void ratio. The shape and extension of the pore–spaces, however, may change during the drying process of SEM sample fabrication (see **Section 3.6**), owing to the development of tensile stresses within the soil fabric during desiccation. As a result of rubber inclusion ($NR_{20}P_0$), the extent of the inter–assemblage pore–spaces were slightly reduced, which can be attributed to the role of rubber particles acting as physical anchors within the soil fabric, thus interlocking neighboring aggregates and withstanding tensile stresses developed during desiccation. However, as long as the rubber particles are relatively larger in size compared with the clay particles, the micro–fabric of the compacted soil–rubber mixture still includes a number of intra–assemblage pore–spaces, owing to the inconsistency in arrangement of the soil–rubber mixture's constituents (see **Figure 14b**). Treating the natural soil with PC ($NR_0P_{0.2}$) resulted in the formation of large uniform aggregates with relatively small intra–assemblage pore–spaces, indicating that the polymer solution could effectively sip into the soil's micro–fabric, and thus bond the clay aggregates together. The larger clay aggregates with less number of intra–assemblage pore–spaces are less prone to water infiltration, which in turn mitigates the swelling behavior of the soil (see **Figure 14c**). Once the soil is included with rubber particles and treated with PC ($NR_{20}P_{0.2}$), the connection interface between the rubber particles and the clay matrices is markedly improved. In micro view, the addition of polymer contributes to the formation of composite aggregates, with rubber particles embedded within the clay aggregates (see the clothed rubber particles in **Figure 14d**). This improves the stability of the compacted soil–rubber mixture against wetting and drying cycles, as the rubber particles contribute to the shear strength of the mixture by providing tensile strength between the clay aggregates and the polymer solution improves the bonding quality of the rubber particles with the clay aggregates; therefore, harnessing the swelling potential of the soil subjected to desiccation cycles (see **Figure 14d**).

## 5. Conclusions

The following conclusions can be drawn from this study:

- As a result of rubber inclusion and/or PC–treatment, the swell–time locus experienced a major downward shift over the semi–log space, indicating a capacity of counteracting the heave in both magnitude and time. The variations of swelling pressure followed a trend

Accepted manuscript doi:
10.1680/jgein.18.00009

similar to that observed for swelling potential, meaning that the higher the rubber content the greater the reduction in swelling potential and swelling pressure, with PC–treated mixtures holding a notable advantage over similar untreated cases.

- Based on common expansive soil classification criteria, i.e. the conventional oedometer swell test and the shrink–swell index, a rubber inclusion of 20% by dry weight of soil (preferably paired with 0.2 g/l PC) would be required to mitigate the swelling problem of South Australian expansive soils.
- The beneficial effects of rubber inclusion and PC–treatment in counteracting the swell–shrink related volume changes were fairly preserved under the influence of alternate wetting and drying. The blending of rubber particles and soil grains, obtained by compaction, could potentially be compromised during wetting and drying. As a result of PC–treatment, however, the interlocking of rubber particles and soil grains, enhanced by the polymer binder, remained intact during successive cycles.
- The rubber inclusions were able to amend desiccation–induced cracking. In this case, the higher the rubber content the greater the improvement in cracking intensity, with PC–treated mixtures holding a slight advantage over similar untreated cases.

**Acknowledgements**

Funding support provided by the Australian Research Council (ARC) via project No. **DP140103004** is gratefully acknowledged.

## NOTATION

Basic SI units are given in parentheses.

| | |
|---|---|
| $C_c$ | coefficient of curvature (dimensionless) |
| **CIF** | crack intensity factor (%) |
| $C_{ps}$ | primary swelling rate (dimensionless) |
| **CRF** | crack reduction factor (%) |
| $C_{ss}$ | secondary swelling rate (dimensionless) |
| $C_u$ | coefficient of uniformity (dimensionless) |
| $d_{10}$ | particle diameter corresponding to 10% finer (m) |
| $d_{30}$ | particle diameter corresponding to 30% finer (m) |
| $d_{50}$ | particle diameter corresponding to 50% finer (m) |
| $d_{60}$ | particle diameter corresponding to 60% finer (m) |
| $d_{90}$ | particle diameter corresponding to 90% finer (m) |
| $e_0$ | initial void ratio (dimensionless) |

Accepted manuscript doi:
10.1680/jgein.18.00009

| | |
|---|---|
| **FSR** | free swell ratio (dimensionless) |
| $G_{sm}$ | specific gravity of soil–rubber mixture (dimensionless) |
| $I_{ss}$ | shrink–swell index (%$Pa^{-1}$) |
| ***LL*** | liquid limit (%) |
| ***LS*** | linear shrinkage (%) |
| ***n*** | number of wetting–drying cycle (dimensionless) |
| ***PI*** | plasticity index (%) |
| ***PL*** | plastic limit (%) |
| $P_s$ | swelling pressure (Pa) |
| $R_c$ | rubber content by dry weight of soil (%) |
| $S_p$ | swelling potential (%) |
| $S_p(n)$ | swelling potential with respect to the $n^{th}$ wetting–drying cycle (%) |
| ***t*** | elapsed time of swelling (s) |
| $t_{is}$ | completion time of the initial swelling phase (s) |
| $t_{ps}$ | completion time of the primary swelling phase (s) |
| $t_{ss}$ | completion time of the secondary swelling phase (s) |
| $\gamma_{dmax}$ | maximum dry unit weight (N/$m^3$) |
| $\varepsilon_a(t)$ | axial swelling strain with respect to elapsed time *t* (%) |
| $\varepsilon_{ais}$ | initial swelling strain (%) |
| $\varepsilon_{aps}$ | primary swelling strain (%) |
| $\varepsilon_{ass}$ | secondary swelling strain (%) |
| $\varepsilon_{sh}$ | ultimate shrinkage strain with respect to the shrink–swell index test (%) |
| $\varepsilon_{sw}$ | ultimate swelling strain with respect to the shrink–swell index test (%) |
| $\omega_{opt}$ | optimum moisture content (%) |

## ABBREVIATIONS

| | |
|---|---|
| **CH** | clay with high plasticity |
| $\mathbf{E^R}$ | extremely reactive |
| **H** | highly expansive |
| $\mathbf{H^R}$ | highly reactive |
| **L** | lowly expansive |
| **M** | moderately expansive |
| $\mathbf{M^R}$ | moderately reactive |
| **PC** | polymer |
| **pF** | potential of free energy (a unit for soil suction) |
| **SEM** | scanning electron microscopy |
| $\mathbf{S^R}$ | slightly reactive |
| **USCS** | unified soil classification system |
| **VH** | very highly expansive |

Accepted manuscript doi:
10.1680/jgein.18.00009

## References

Akbulut, S., Arasan, S. & Kalkan, E. (**2007**). Modification of clayey soils using scrap tire rubber and synthetic fibers. *Applied Clay Science*, **38**, No. 1–2, 23–32, http://dx.doi.org/10.1016/j.clay.2007.02.001.

Al-Akhras, N. M., Attom, M. F., Al-Akhras, K. M. & Malkawi, A. I. H. (**2008**). Influence of fibers on swelling properties of clayey soil. *Geosynthetics International*, **15**, No. 4, 304–309, http://dx.doi.org/10.1680/gein.2008.15.4.304.

Alazigha, D. P., Indraratna, B., Vinod, J. S. & Ezeajugh, L. E. (**2016**). The swelling behaviour of lignosulfonate–treated expansive soil. *Proceedings of the Institution of Civil Engineers–Ground Improvement*, **169**, No.3, 182–193, http://dx.doi.org/10.1680/jgrim.15.00002.

Alonso, E. E., Romero, E., Hoffmann, C. & García-Escudero, E. (**2005**). Expansive bentonite–sand mixtures in cyclic controlled–suction drying and wetting. *Engineering Geology*, **81**, No.3, 213–226, http://dx.doi.org/10.1016/j.enggeo.2005.06.009.

Al-Rawas, A. A., Hago, A. W. & Al-Sarmi, H. (**2005**). Effect of lime, cement and Sarooj (artificial pozzolan) on the swelling potential of an expansive soil from Oman. *Building and Environment*, **40**, No.5, 681–687, http://dx.doi.org/10.1016/j.buildenv.2004.08.028.

Andrews, R. & Sharp, K. (**2010**). A protocol for conducting field trials for best value management of unsealed roads. *Proceedings of the 24th ARRB Conference–Building on 50 Years of Road and Transport Research*, ARRB, Melbourne, Victoria, Australia, October 2010, pp. 1–14.

Arulrajah, A., Kua, T. A., Horpibulsuk, S., Mirzababaei, M. & Chinkulkijniwat, A. (**2017[b]**). Recycled glass as a supplementary filler material in spent coffee grounds geopolymers. *Construction and Building Materials*, **151**, 18–27, http://dx.doi.org/10.1016/j.conbuildmat.2017.06.050.

Arulrajah, A., Kua, T. A., Suksiripattanapong, C., Horpibulsuk, S. & Shen, J. S. (**2017[a]**). Compressive strength and microstructural properties of spent coffee grounds–bagasse ash based geopolymers with slag supplements. *Journal of Cleaner Production*, **162**, 1491–1501, http://dx.doi.org/10.1016/j.jclepro.2017.06.171.

Arulrajah, A., Mohammadinia, A., D'Amico, A. & Horpibulsuk, S. (**2017[c]**). Effect of lime kiln dust as an alternative binder in the stabilization of construction and demolition materials. *Construction and Building Materials*, **152**, 999–1007, http://dx.doi.org/10.1016/j.conbuildmat.2017.07.070.

AS 1289.3.2.1:09. Methods of testing soils for engineering purposes: Soil classification tests – Determination of the plastic limit of a soil. *Standards Australia*, Sydney, New South Wales, Australia.

AS 1289.3.3.1:09 . Methods of testing soils for engineering purposes: Soil classification tests – Calculation of the plasticity index of a soil. *Standards Australia*, Sydney, New South Wales, Australia.

AS 1289.3.4.1:08. Methods of testing soils for engineering purposes: Soil classification tests – Determination of the linear shrinkage of a soil. *Standards Australia*, Sydney, New South Wales, Australia.

AS 1289.3.9.1:15. Methods of testing soils for engineering purposes: Soil classification tests – Determination of the cone liquid limit of a soil. *Standards Australia*, Sydney, New South Wales, Australia.

AS 1289.7.1.1:03. Methods of testing soils for engineering purposes: Soil reactivity tests – Determination of the shrinkage index of a soil – Shrink–swell index. *Standards Australia*, Sydney, New South Wales, Australia.

AS 2870:11. Residential slabs and footings. *Standards Australia*, Sydney, New South Wales, Australia.

ASTM D2487-11. Standard practice for classification of soils for engineering purposes (Unified Soil Classification System). *ASTM International*, West Conshohocken, Pennsylvania, USA, http://dx.doi.org/10.1520/d2487-11.

ASTM D422-63(2007)e2. Standard test method for particle–size analysis of soils. *ASTM International*, West Conshohocken, Pennsylvania, USA, http://dx.doi.org/10.1520/d0422-63r07e02.

ASTM D4546-14. Standard test methods for one–dimensional swell or collapse of soils. *ASTM International*, West Conshohocken, Pennsylvania, USA, http://dx.doi.org/10.1520/d4546.

ASTM D698-12e2. Standard test methods for laboratory compaction characteristics of soil using standard effort (12,400 ft–lbf/ft$^3$ (600 kN–m/m$^3$)). *ASTM International*, West Conshohocken, Pennsylvania, USA, http://dx.doi.org/10.1520/d0698-12e02.

ASTM D854-14. Standard test methods for specific gravity of soil solids by water pycnometer. *ASTM International*, West Conshohocken, Pennsylvania, USA, http://dx.doi.org/10.1520/d0854-14.

Ayeldeen, M. & Kitazume, M. (**2017**). Using fiber and liquid polymer to improve the behaviour of cement–stabilized soft clay. *Geotextiles and Geomembranes*, **45**, No.6, 592–602, http://dx.doi.org/10.1016/j.geotexmem.2017.05.005.

Basma, A. A., Al-Homoud, A. S., Malkawi, A. I. H. & Al-Bashabsheh, M. A. (**1996**). Swelling–shrinkage behavior of natural expansive clays. *Applied Clay Science*, **11**, No. 2–4, 211–227, http://dx.doi.org/10.1016/s0169-1317(96)00009-9.

Camarena, S. (**2013**). Sustainable road maintenance and construction utilising new technologies. *Proceedings of the IPWEA International Public Works Conference*, IPWEA, Darwin, Northern Territory, Australia, August 2013, pp. 1–11.

Cameron, D. A. (**1989**). Tests for reactivity and prediction of ground movement. *Civil Engineering Transactions/The Institution of Engineers, Australia*, **31**, No. 3, 121–132.

Cameron, D. A. (**2001**). The extent of soil desiccation near trees in a semi–arid environment. *Geotechnical and Geological Engineering*, **19**, No.3–4, 357–370, http://dx.doi.org/10.1023/a:1013168708654.

Cetin, H., Fener, M. & Gunaydin, O. (**2006**). Geotechnical properties of tire–cohesive clayey soil mixtures as a fill material. *Engineering Geology*, **88**, No. 1–2, 110–120, http://dx.doi.org/10.1016/j.enggeo.2006.09.002.

Chaduvula, U., Viswanadham, B. V. S. & Kodikara, J. (**2017**). A study on desiccation cracking behavior of polyester fiber–reinforced expansive clay. *Applied Clay Science*, **142**, 163–172, http://dx.doi.org/10.1016/j.clay.2017.02.008.

Costa, S., Kodikara, J. & Shannon, B. (**2013**). Salient factors controlling desiccation cracking of clay in laboratory experiments. *Géotechnique*, **63**, No. 1, 18–29, http://dx.doi.org/10.1680/geot.9.p.105.

De Camillis, M., Di Emidio, G., Bezuijen, A., Flores, D. V., Stappen, J. V. & Cnudde, V. (**2017**). Effect of wet–dry cycles on polymer treated bentonite in seawater: Swelling ability, hydraulic conductivity and crack analysis. *Applied Clay Science*, **142**, 52–59, http://dx.doi.org/10.1016/j.clay.2016.11.011.

Dif, A. & Bluemel, W. (**1991**). Expansive soils under cyclic drying and wetting. *Geotechnical Testing Journal*, **14**, No. 1, 96–102, http://dx.doi.org/10.1520/gtj10196j.

Estabragh, A. R., Parsaei, B. & Javadi, A. A. (**2015**). Laboratory investigation of the effect of cyclic wetting and drying on the behaviour of an expansive soil. *Soils and Foundations*, **55**, No. 2, 304–314, http://dx.doi.org/10.1016/j.sandf.2015.02.007.

Estabragh, A. R., Pereshkafti, M. R. S., Parsaei, B. & Javadi, A. A. (**2013**). Stabilised expansive soil behaviour during wetting and drying. *International Journal of Pavement Engineering*, **14**, No. 4, 418–427, http://dx.doi.org/10.1080/10298436.2012.746688.

Estabragh, A. R., Rafatjo, H. & Javadi, A. A. (**2014**). Treatment of an expansive soil by mechanical and chemical techniques. *Geosynthetics International*, **21**, No. 3, 233–243, http://dx.doi.org/10.1680/gein.14.00011.

Fityus, S. G., Cameron, D. A. & Walsh, P. F. (**2005**). The shrink swell test. *Geotechnical Testing Journal*, **28**, No. 1, 92–101, http://dx.doi.org/10.1520/gtj12327.

Georgees, R. N., Hassan, R. A., Evans, R. P. & Jegatheesan, P. (**2015**). Effect of the use of a polymeric stabilizing additive on unconfined compressive strength of soils. *Transportation Research Record: Journal of the Transportation Research Board*, **2473**, 200–208, http://dx.doi.org/10.3141/2473-23.

Graber, E. R., Fine, P. & Levy, G. J. (**2006**). Soil stabilization in semiarid and arid land agriculture. *Journal of Materials in Civil Engineering*, **18**, No. 2, 190–205, http://dx.doi.org/10.1061/(asce)0899-1561(2006)18:2(190).

Guney, Y., Sari, D., Cetin, M. & Tuncan, M. (**2007**). Impact of cyclic wetting–drying on swelling behavior of lime–stabilized soil. *Building and Environment*, **42**, No. 2, 681–688, http://dx.doi.org/10.1016/j.buildenv.2005.10.035.

Hannam, P. (**2014**). Tyre industry divided over how to handle toxic waste. *The Sydney Morning Herald*, Sydney, New South Wales, Australia. See http://www.smh.com.au/environment/tyre-industry-divided-over-how-to-handle-toxic-waste-20140120-314ic.html (accessed 12/12/2017)

Holtz, W. G. & Gibbs, H. J. (**1956**). Engineering properties of expansive clays. *Transactions of the American Society of Civil Engineers*, **121**, No. 1, 641–663.

Hoyos, L. R., Chainuwat, P. & Puppala, A. J. (**2006**). Dynamic characterization of chemically modified expansive soil. In: *Expansive Soils: Recent Advances in Characterization and Treatment*, Al-Rawas, A. A. & Goosen, M. F. A., Eds., Taylor & Francis Group, London, UK, pp. 465–481, http://dx.doi.org/10.1201/9780203968079.ch32.

Inyang, H. I., Bae, S., Mbamalu, G. & Park, S. (**2007**). Aqueous polymer effects on volumetric swelling of Na–Montmorillonite. *Journal of Materials in Civil Engineering*, **19**, No. 1, 84–90, http://dx.doi.org/10.1061/(asce)0899-1561(2007)19:1(84).

Kalkan, E. (**2011**). Impact of wetting–drying cycles on swelling behavior of clayey soils modified by silica fume. *Applied Clay Science*, **52**, No. 4, 345–352, http://dx.doi.org/10.1016/j.clay.2011.03.014.

Kalkan, E. (**2013**). Preparation of scrap tire rubber fiber–silica fume mixtures for modification of clayey soils. *Applied Clay Science*, **80**–**81**, 117–125, http://dx.doi.org/10.1016/j.clay.2013.06.014.

Kim, S. & Palomino, A. M. (**2009**). Polyacrylamide–treated kaolin: A fabric study. *Applied Clay Science*, **45**, No.4, 270–279, http://dx.doi.org/10.1016/j.clay.2009.06.009.

Kodikara, J. & Chakrabarti, S. (**2005**). Modeling of moisture loss in cementitiously stabilized pavement materials. *International Journal of Geomechanics*, **5**, No. 4, 295–303, http://dx.doi.org/10.1061/(asce)1532-3641(2005)5:4(295).

Konrad, J. M. & Ayad, R. (**1997**). A idealized framework for the analysis of cohesive soils undergoing desiccation. *Canadian Geotechnical Journal*, **34**, No. 4, 477–488, http://dx.doi.org/10.1139/t97-015.

Kua, T. A., Arulrajah, A., Mohammadinia, A., Horpibulsuk, S. & Mirzababaei, M. (**2017**). Stiffness and deformation properties of spent coffee grounds based geopolymers. *Construction and Building Materials*, **138**, 79–87, http://dx.doi.org/10.1016/j.conbuildmat.2017.01.082.

Laird, D. A. (**1997**). Bonding between polyacrylamide and clay mineral surfaces. *Soil Science*, **162**, No. 11, 826–832, http://dx.doi.org/10.1097/00010694-199711000-00006.

Letey, J. (**1994**). Adsorption and desorption of polymers on soil. *Soil Science*, **158**, No. 4, 244–248, http://dx.doi.org/10.1097/00010694-199410000-00003.

Lu, J. H., Wu, L. & Letey, J. (**2002**). Effects of soil and water properties on anionic polyacrylamide sorption. *Soil Science Society of America Journal*, **66**, No. 2, 578–584, http://dx.doi.org/10.2136/sssaj2002.5780.

Miller, C. J. & Rifai, S. (**2004**). Fiber reinforcement for waste containment soil liners. *Journal of Environmental Engineering*, **130**, No. 8, 891–895, http://dx.doi.org/10.1061/(asce)0733-9372(2004)130:8(891).

Miller, W. P., Willis, R. L. & Levy, G. J. (**1998**). Aggregate stabilization in kaolinitic soils by low rates of anionic polyacrylamide. *Soil Use and Management*, **14**, No. 2, 101–105, http://dx.doi.org/10.1111/j.1475-2743.1998.tb00623.x.

Mirzababaei, M., Miraftab, M., Mohamed, M. & McMahon, P. (**2013**[a]). Impact of carpet waste fibre addition on swelling properties of compacted clays. *Geotechnical and Geological Engineering*, **31**, No. 1, 173–182, http://dx.doi.org/10.1007/s10706-012-9578-2.

Mirzababaei, M., Miraftab, M., Mohamed, M. & McMahon, P. (**2013**[b]). Unconfined compression strength of reinforced clays with carpet waste fibers. *Journal of Geotechnical and Geoenvironmental Engineering*, **139**, No. 3, 483–493, http://dx.doi.org/10.1061/(asce)gt.1943-5606.0000792.

Mirzababaei, M., Mohamed, M. & Miraftab, M. (**2017**[b]). Analysis of strip footings on fiber–reinforced slopes with the aid of particle image velocimetry. *Journal of Materials in Civil Engineering*, **29**, No. 4, 04016243:1–04016243:14. http://dx.doi.org/10.1061/(asce)mt.1943-5533.0001758.

Mirzababaei, M., Mohamed, M., Arulrajah, A., Horpibulsuk, S. & Anggraini, V. (**2017[a]**). Practical approach to predict the shear strength of fibre–reinforced clay. *Geosynthetics International*, **in press**, http://dx.doi.org/10.1680/jgein.17.00033.

Mirzababaei, M., Yasrobi, S. S. & Al-Rawas, A. A. (**2009**). Effect of polymers on swelling potential of expansive soils. *Proceedings of the Institution of Civil Engineers–Ground Improvement*, **162**, No. 3, 111–119, http://dx.doi.org/10.1680/grim.2009.162.3.111.

Mitchell, J. K. & Soga, K. (**2005**). Fundamentals of soil behavior (3rd Ed.). John Wiley & Sons, Hoboken, New Jersey, USA, 592 pp.

Nahlawi, H. & Kodikara, J. K. (**2006**). Laboratory experiments on desiccation cracking of thin soil layers. *Geotechnical and Geological Engineering*, **24**, No. 6, 1641–1664, http://dx.doi.org/10.1007/s10706-005-4894-4.

Onyejekwe, S. & Ghataora, G. S. (**2015**). Soil stabilization using proprietary liquid chemical stabilizers: Sulphonated oil and a polymer. *Bulletin of Engineering Geology and the Environment*, **74**, No. 2, 651–665, http://dx.doi.org/10.1007/s10064-014-0667-8.

Özkul, Z. H. & Baykal, G. (**2007**). Shear behavior of compacted rubber fiber–clay composite in drained and undrained loading. *Journal of Geotechnical and Geoenvironmental Engineering*, **133**, No. 7, 767–781, http://dx.doi.org/10.1061/(asce)1090-0241(2007)133:7(767).

Patil, U., Valdes, J. R. & Evans, T. M. (**2011**). Swell mitigation with granulated tire rubber. *Journal of Materials in Civil Engineering*, **23**, No. 5, 721–727, http://dx.doi.org/10.1061/(asce)mt.1943-5533.0000229.

Phanikumar, B. R. & Singla, R. (**2016**). Swell–consolidation characteristics of fibre–reinforced expansive soils. *Soils and Foundations*, **56**, No. 1, 138–143, http://dx.doi.org/10.1016/j.sandf.2016.01.011.

Phummiphan, I., Horpibulsuk, S., Rachan, R., Arulrajah, A., Shen, S. L. & Chindaprasirt, P. (**2018**). High calcium fly ash geopolymer stabilized lateritic soil and granulated blast furnace slag blends as a pavement base material. *Journal of Hazardous Materials*, **341**, 257–267, http://dx.doi.org/10.1016/j.jhazmat.2017.07.067.

Prakash, K. & Sridharan, A. (**2004**). Free swell ratio and clay mineralogy of fine–grained soils. *Geotechnical Testing Journal*, **27**, No.2, 220–225, http://dx.doi.org/10.1520/gtj10860.

Puppala, A. J., Griffin, J. A., Hoyos, L. R. & Chomtid, S. (**2004**). Studies on sulfate–resistant cement stabilization methods to address sulfate–induced soil heave. *Journal of Geotechnical and Geoenvironmental Engineering*, **130**, No. 4, 391–402, http://dx.doi.org/10.1061/(asce)1090-0241(2004)130:4(391).

Rabiee, A., Gilani, M., Jamshidi, H. & Baharvand, H. (**2013**). Synthesis and characterization of a calcium– and sodium–containing acrylamide–based polymer and its effect on soil strength. *Journal of Vinyl and Additive Technology*, **19**, No. 2, 140–146, http://dx.doi.org/10.1002/vnl.21310.

Rao, S. M., Reddy, B. V. V. & Muttharam, M. (**2001**). The impact of cyclic wetting and drying on the swelling behavior of stabilized expansive soils. *Engineering Geology*, **60**, No. 1–4, 223–233, http://dx.doi.org/10.1016/s0013-7952(00)00103-4.

Rao, S. M., Thyagaraj, T. & Thomas, H. R. (**2006**). Swelling of compacted clay under osmotic gradients. *Géotechnique*, **56**, No. 10, 707–713, http://dx.doi.org/10.1680/geot.2006.56.10.707.

Rauch, A., Harmon, J., Katz, L. & Liljestrand, H. (**2002**). Measured effects of liquid soil stabilizers on engineering properties of clay. *Transportation Research Record: Journal of the Transportation Research Board*, **1787**, 33–41, http://dx.doi.org/10.3141/1787-04.

Seda, J. H., Lee, J. C. & Carraro, J. A. H. (**2007**). Beneficial use of waste tire rubber for swelling potential mitigation in expansive soils. In: *Geo-Denver 2007: Soil Improvement (GSP 172)*, Schaefer, V. R., Filz, G. M., Gallagher, P. M., Sehn, A. L. & Wissmann, K. J., Eds., ASCE, Denver, Colorado, USA, pp. 1–9, http://dx.doi.org/10.1061/40916(235)5.

Seddon, K. D. (**1992**). Reactive soils. In: *Engineering Geology of Melbourne*, Peck, W. A., Neilson, J. L., Olds, R. J. & Seddon, K. D. Eds., A.A. Balkema, Melbourne, Victoria, Australia, pp. 33–37.

Seed, H. B., Woodward, J. & Lundgren, R. (**1962**). Prediction of swelling potential for compacted clays. *Journal of the Soil Mechanics and Foundations Division*, **88**, No. 3, 53–88.

Seybold, C. A. (**1994**). Polyacrylamide review: Soil conditioning and environmental fate. *Communications in Soil Science and Plant Analysis*, **25**, No. 11–12, 2171–2185, http://dx.doi.org/10.1080/00103629409369180.

Signes, C. H., Garzón-Roca, J., Fernández, P. M., Torre, M. E. G. & Franco, R. I. (**2016**). Swelling potential reduction of Spanish argillaceous marlstone Facies Tap soil through the addition of crumb rubber particles from scrap tyres. *Applied Clay Science*, **132**–**133**, 768–773, http://dx.doi.org/10.1016/j.clay.2016.07.027.

Sivapullaiah, P. V., Sridharan, A. & Ramesh, H. N. (**2000**). Strength behaviour of lime–treated soils in the presence of sulphate. *Canadian Geotechnical Journal*, **37**, No. 6, 1358–1367, http://dx.doi.org/10.1139/t00-052.

Sivapullaiah, P. V., Sridharan, A. & Stalin, V. K. (**1996**). Swelling behaviour of soil–bentonite mixtures. *Canadian Geotechnical Journal*, **33**, No. 5, 808–814, http://dx.doi.org/10.1139/t96-106-326.

Soltani, A., Deng, A. & Taheri, A. (**2018**). Swell–compression characteristics of a fiber–reinforced expansive soil. *Geotextiles and Geomembranes*, **46**, No. 2, 183–189, http://dx.doi.org/10.1016/j.geotexmem.2017.11.009.

Soltani, A., Deng, A., Taheri, A. & Mirzababaei, M. (**2017**[**b**]). A sulphonated oil for stabilisation of expansive soils. *International Journal of Pavement Engineering*, **in press**, http://dx.doi.org/10.1080/10298436.2017.1408270.

Soltani, A., Taheri, A., Khatibi, M. & Estabragh, A. R. (**2017**[**a**]). Swelling potential of a stabilized expansive soil: A comparative experimental study. *Geotechnical and Geological Engineering*, **35**, No. 4, 1717–1744, http://dx.doi.org/10.1007/s10706-017-0204-1.

Sridharan, A. & Gurtug, Y. (**2004**). Swelling behaviour of compacted fine–grained soils. *Engineering Geology*, **72**, No. 1, 9–18, http://dx.doi.org/10.1016/s0013-7952(03)00161-3.

Sridharan, A. & Keshavamurthy, P. (**2016**). Expansive soil characterisation: An appraisal. *INAE Letters*, **1**, No. 1, 29–33, http://dx.doi.org/10.1007/s41403-016-0001-9.

Sridharan, A. & Prakash, K. (**2000**). Classification procedures for expansive soils. *Proceedings of the Institution of Civil Engineers–Geotechnical Engineering*, **143**, No. 4, 235–240, http://dx.doi.org/10.1680/geng.2000.143.4.235.

Sridharan, A., Rao, A. & Sivapullaiah, P. (**1986**). Swelling pressure of clays. *Geotechnical Testing Journal*, **9**, No. 1, 24–33, http://dx.doi.org/10.1520/gtj10608j.

Srivastava, A., Pandey, S. & Rana, J. (**2014**). Use of shredded tyre waste in improving the geotechnical properties of expansive black cotton soil. *Geomechanics and Geoengineering*, **9**, No.4, 303–311, http://dx.doi.org/10.1080/17486025.2014.902121.

Suksiripattanapong, C., Kua, T. A., Arulrajah, A., Maghool, F. & Horpibulsuk, S. (**2017**). Strength and microstructure properties of spent coffee grounds stabilized with rice husk ash and slag geopolymers. *Construction and Building Materials*, **146**, 312–320, http://dx.doi.org/10.1016/j.conbuildmat.2017.04.103.

Tang, C. S., Shi, B. & Zhao, L. Z. (**2010**). Interfacial shear strength of fiber reinforced soil. *Geotextiles and Geomembranes*, **28**, No. 1, 54–62, http://dx.doi.org/10.1016/j.geotexmem.2009.10.001.

Tang, C. S., Shi, B., Cui., Y. J., Liu, C. & Gua, K. (**2012**). Desiccation cracking behavior of polypropylene fiber–reinforced clayey soil. *Canadian Geotechnical Journal*, **49**, No. 9, 1088–1101, http://dx.doi.org/10.1139/t2012-067.

Tang, C. S., Shi, B., Gao, W., Chen, F. & Cai, Y. (**2007**). Strength and mechanical behavior of short polypropylene fiber reinforced and cement stabilized clayey soil. *Geotextiles and Geomembranes*, **25**, No. 3, 194–202, http://dx.doi.org/10.1016/j.geotexmem.2006.11.002.

Theng, B. K. G. (**1982**). Clay–polymer interactions: Summary and perspectives. *Clays and Clay Minerals*, **30**, No. 1, 1–10, http://dx.doi.org/10.1346/ccmn.1982.0300101.

Tripathy, S., Subba Rao, K. S. & Fredlund, D. G. (**2002**). Water content–void ratio swell–shrink paths of compacted expansive soils. *Canadian Geotechnical Journal*, **39**, No.4, 938–959, http://dx.doi.org/10.1139/t02-022.

Trouzine, H., Bekhiti, M. & Asroun, A. (**2012**). Effects of scrap tyre rubber fibre on swelling behaviour of two clayey soils in Algeria. *Geosynthetics International*, **19**, No. 2, 124–132, http://dx.doi.org/10.1680/gein.2012.19.2.124.

Viswanadham, B. V. S., Phanikumar, B. R. & Mukherjee, R. V. (**2009[b]**). Effect of polypropylene tape fibre reinforcement on swelling behaviour of an expansive soil. *Geosynthetics International*, **16**, No. 5, 393–401, http://dx.doi.org/10.1680/gein.2009.16.5.393.

Viswanadham, B. V. S., Phanikumar, B. R. & Mukherjee, R. V. (**2009[a]**). Swelling behaviour of a geofiber–reinforced expansive soil. *Geotextiles and Geomembranes*, **27**, No. 1, 73–76, http://dx.doi.org/10.1016/j.geotexmem.2008.06.002.

Wallace, A., Wallace, G. A. & Cha, W. J. (**1986**). Mechanisms involved in soil conditioning by polymers. *Soil Science*, **141**, No. 5, 381–386, http://dx.doi.org/10.1097/00010694-198605000-00017.

Wray, W. K. (**1998**). Mass transfer in unsaturated soils: A review of theory and practices. *Proceedings of the 2nd International Conference on Unsaturated Soils (Unsat 98)*, International Academic Publishing House, Beijing, China, August 1998, pp. 99–155.

Wroth, C. P. & Wood, D. M. (**1978**). The correlation of index properties with some basic engineering properties of soils. *Canadian Geotechnical Journal*, **15**, No.2, 137–145, http://dx.doi.org/10.1139/t78-014.

Yadav, J. S. & Tiwari, S. K. (**2017[a]**). Effect of waste rubber fibres on the geotechnical properties of clay stabilized with cement. *Applied Clay Science*, **149**, 97–110, http://dx.doi.org/10.1016/j.clay.2017.07.037.

Yadav, J. S. & Tiwari, S. K. (**2017[b]**). The impact of end–of–life tires on the mechanical properties of fine–grained soil: A Review. *Environment, Development and Sustainability*, **in press**, http://dx.doi.org/10.1007/s10668-017-0054-2.

Yazdandoust, F. & Yasrobi, S. S. (**2010**). Effect of cyclic wetting and drying on swelling behavior of polymer–stabilized expansive clays. *Applied Clay Science*, **50**, No. 4, 461–468, http://dx.doi.org/10.1016/j.clay.2010.09.006.

Yesiller, N., Miller, C. J., Inci, G. & Yaldo, K. (**2000**). Desiccation and cracking behavior of three compacted landfill liner soils. *Engineering Geology*, **57**, No. 1–2, 105–121, http://dx.doi.org/10.1016/s0013-7952(00)00022-3.

Zhang, R., Yang, H. & Zheng, J. (**2006**). The effect of vertical pressure on the deformation and strength of expansive soil during cyclic wetting and drying. In: *Unsaturated Soils 2006*, Miller, G. A., Zapata, C. E., Houston, S. L. & Fredlund, D. G., Eds., ASCE, Carefree, Arizona, USA, pp. 894–905, http://dx.doi.org/10.1061/40802(189)71.

Accepted manuscript doi:
10.1680/jgein.18.00009

**Table 1.** Physical and mechanical properties of the soil.

| Properties | Value | Standard designation |
|---|---|---|
| Specific gravity, $G_s$ | 2.76 | ASTM D854 |
| ***Grain–size distribution*** | | |
| Clay (<2 μm) (%) | 44 | |
| Silt (2–75 μm) (%) | 36 | |
| Fine sand (0.075–0.425 mm) | 15 | ASTM D422 |
| Medium sand (0.425–2 mm) | 4 | |
| Coarse sand (2–4.75 mm) | 1 | |
| ***Consistency limits*** | | |
| Liquid limit, *LL* (%) | 78.04 | AS 1289.3.9.1 |
| Plastic limit, *PL* (%) | 22.41 | AS 1289.3.2.1 |
| Plasticity index, *PI* (%) | 55.63 | AS 1289.3.3.1 |
| Linear shrinkage, *LS* (%) | 15.78 | AS 1289.3.4.1 |
| USCS soil classification | CH | ASTM D2487 |
| ***Swelling properties*** | | |
| Swelling potential, $S_p$ (%) † | 10.68 | ASTM D4546 |
| Swelling pressure, $P_s$ (kPa) | 235 | |
| Free swell ratio, FSR ‡ | 2.27 | Sridharan and Prakash (2000) |
| ***Compaction characteristics*** | | |
| Maximum dry unit weight, $\gamma_{dmax}$ (kN/m$^3$) | 15.9 | ASTM D698 |
| Optimum moisture content, $\omega_{opt}$ (%) | 21.0 | |

**Notes:**
† % expansion in oedometer from optimum moisture content to saturated condition under $\sigma'_0$=7 kPa; and ‡ ratio of equilibrium sediment volume of 10 g oven–dried soil passing sieve 425 μm in distilled water to that of kerosene.

Accepted manuscript doi:
10.1680/jgein.18.00009

**Table 2.** Physical properties and chemical composition of tire rubber powder (as supplied by the manufacturer).

| **Properties** | **Value/Description** |
|---|---|
| ***Physical properties*** | |
| Physical appearance | Fine black powder |
| Solubility in water | Insoluble |
| Water adsorption | Negligible |
| Resistance to acid and alkaline | Excellent |
| Specific gravity (at 20$^{o}$C), $G_s$ | 1.09 |
| Softening point ($^{o}$C) | 170 |
| ***Chemical composition*** | |
| Styrene–Butadiene copolymer (%) | 55 |
| Acetone extract (%) | 5–20 |
| Carbon black (%) | 25–35 |
| Zinc oxide (%) | 2.5 |
| Sulphur (%) | 1–3 |

**Table 3.** Mix designs and their properties used for the main experimental program.

| **Soil (%)** | **$R_c$ (%)** | **PC (g/l)** | **Designation** | ***LL* (%)** † | **$\omega_{opt}$ (%)** ‡ | **$\gamma_{dmax}$ (kN/m$^3$)** ‡ | **$G_{sm}$** * | **$e_0$** ‡ |
|---|---|---|---|---|---|---|---|---|
| 100 | 0 | 0 | $NR_0P_0$ | 78.04 | 21.0 | 15.9 | 2.76 | 0.706 |
| 90 | 10 | | $NR_{10}P_0$ | 73.32 | 18.1 | 15.4 | 2.42 | 0.538 |
| 80 | 20 | | $NR_{20}P_0$ | 68.59 | 16.5 | 15.2 | 2.20 | 0.422 |
| 70 | 30 | | $NR_{30}P_0$ | 65.58 | 15.0 | 14.7 | 2.04 | 0.359 |
| 100 | 0 | 0.2 | $NR_0P_{0.2}$ | 87.61 | 22.0 | 16.2 | 2.76 | 0.668 |
| 90 | 10 | | $NR_{10}P_{0.2}$ | 83.67 | 18.9 | 15.6 | 2.42 | 0.524 |
| 80 | 20 | | $NR_{20}P_{0.2}$ | 77.73 | 17.0 | 15.1 | 2.20 | 0.424 |
| 70 | 30 | | $NR_{30}P_{0.2}$ | 72.14 | 15.5 | 14.9 | 2.04 | 0.344 |

**Notes:**
† initial placement condition for desiccation–induced crack tests; ‡ initial placement condition for oedometer swell–compression, soil reactivity (shrink–swell index), cyclic wetting and drying and SEM tests; and * specific gravity of mixtures obtained as per **Equation 2**.

Accepted manuscript doi:
10.1680/jgein.18.00009

**Table 4.** Free swell ratio (FSR) for the natural soil treated with various PC concentrations.

| Mixture | $V_k$ ($cm^3$) | $V_d$ ($cm^3$) | $V_p$ ($cm^3$) | FSR | Degree of expansivity | Classification procedures with respect to FSR (Sridharan and Prakash 2000) | | | | |
|---|---|---|---|---|---|---|---|---|---|---|
| $NR_0P_0$ | 15.0 | 34.0 | — | 2.27 | High | | | | | |
| $NR_0P_{0.2}$ † | 15.0 | — | 25.0 | 1.67 | Moderate | ≤1 | 1–1.5 | 1.5–2 | 2–4 | >4 |
| $NR_0P_{0.4}$ | 15.0 | — | 24.5 | 1.63 | Moderate | Negligible | Low | Moderate | High | Very High |
| $NR_0P_{0.6}$ | 15.0 | — | 23.0 | 1.53 | Moderate | | | | | |

**Notes:**
† manufacturer–recommended concentration; FSR=$V_d/V_k$ or $V_p/V_k$; and $V_k$, $V_d$ and $V_p$=equilibrium sediment volume of 10 g oven–dried soil passing sieve 425 μm in kerosene, distilled water and PC solution, respectively.

**Table 5.** Classification procedures for expansive soils with respect to the oedometer swell test.

| Degree of expansivity | Holtz and Gibbs (1956) † | Seed et al. (1962) ‡ | Sridharan and Prakash (2000) † |
|---|---|---|---|
| Low (L) | <10 | 0–1.5 | 1–5 |
| Moderate (M) | 10–20 | 1.5–5 | 5–15 |
| High (H) | 20–30 | 5–25 | 15–25 |
| Very High (VH) | >30 | >25 | >25 |

**Notes:**
† % expansion in oedometer from air–dry to saturated condition under $\sigma'_0$=7 kPa; and ‡ % expansion in oedometer from optimum moisture content to saturated condition under $\sigma'_0$=7 kPa.

**Table 6.** Classification procedures for expansive soils with respect to the shrink–swell index (Seddon 1992).

| Degree of expansivity/reactivity | Shrink–Swell index, $I_{ss}$ (%$pF^{-1}$) |
|---|---|
| Slightly reactive ($S^R$) | 0.8–1.7 |
| Moderately reactive ($M^R$) | 1.7–3.3 |
| Highly reactive ($H^R$) | 3.3–5.8 |
| Extremely reactive ($E^R$) | >5.8 |

Accepted manuscript doi:
10.1680/jgein.18.00009

**Table 7.** Summary of the swell–time characteristics for the tested samples.

| Mixture | $t_{is}$ (min) | $t_{ps}$ (min) | $\varepsilon_{ais}$ (%) | $\varepsilon_{aps}$ (%) | $\varepsilon_{ass}$ (%) | $S_p$ (%) | $C_{ps}$ ($\times 10^2$) | $C_{ss}$ ($\times 10^3$) |
|---|---|---|---|---|---|---|---|---|
| $NR_0P_0$ | 21 | 939 | 1.40 | 8.00 | 1.27 | 10.68 | 4.85 | 10.71 |
| $NR_{10}P_0$ | 26 | 1161 | 1.11 | 6.46 | 1.03 | 8.60 | 3.92 | 9.38 |
| $NR_{20}P_0$ | 28 | 1167 | 0.95 | 5.38 | 0.93 | 7.26 | 3.32 | 8.53 |
| $NR_{30}P_0$ | 34 | 1441 | 0.74 | 4.28 | 0.71 | 5.73 | 2.63 | 7.06 |
| $NR_0P_{0.2}$ | 18 | 753 | 0.94 | 5.33 | 0.88 | 7.15 | 3.28 | 6.84 |
| $NR_{10}P_{0.2}$ | 29 | 1343 | 0.79 | 4.71 | 0.70 | 6.20 | 2.83 | 6.79 |
| $NR_{20}P_{0.2}$ | 35 | 1412 | 0.54 | 3.20 | 0.53 | 4.28 | 1.99 | 5.30 |
| $NR_{30}P_{0.2}$ | 62 | 2387 | 0.41 | 2.38 | 0.41 | 3.20 | 1.50 | 5.28 |

**Table 8.** Degree of expansivity for the tested samples during wetting and drying cycles.

| Mixture | $n$ | $S_p(n)$ (%) | Degree of expansivity | Degree of expansivity |
|---|---|---|---|---|
| $NR_0P_0$ | 1 | 10.68 | High † | High † |
| | 2 | 13.28 | Moderate ‡ | Moderate * |
| | 3 | 9.23 | Low ‡ | Moderate * |
| | 4 | 7.45 | Low ‡ | Moderate * |
| | 5 | 7.55 | Low ‡ | Moderate * |
| $NR_{30}P_0$ | 1 | 5.73 | High † | High † |
| | 2 | 7.03 | Low ‡ | Moderate * |
| | 3 | 6.63 | Low ‡ | Moderate * |
| | 4 | 6.35 | Low ‡ | Moderate * |
| | 5 | 6.20 | Low ‡ | Moderate * |
| $NR_0P_{0.2}$ | 1 | 7.15 | High † | High † |
| | 2 | 5.10 | Low ‡ | Moderate * |
| | 3 | 4.10 | Low ‡ | Low * |
| | 4 | 3.70 | Low ‡ | Low * |
| | 5 | 3.80 | Low ‡ | Low * |
| $NR_{30}P_{0.2}$ | 1 | 3.20 | Moderate † | Moderate † |
| | 2 | 2.75 | Low ‡ | Low * |
| | 3 | 2.00 | Low ‡ | Low * |
| | 4 | 1.80 | Low ‡ | Low * |
| | 5 | 1.70 | Low ‡ | Low * |

**Notes:**
† classified as per Seed et al. (1962) (see **Table 5**); ‡ classified as per Holtz and Gibbs (1956) (see **Table 5**); and * classified as per Sridharan and Prakash (2000) (see **Table 5**).

Accepted manuscript doi:
10.1680/jgein.18.00009

**Figure 1.** Grain–size distribution curves for the soil and tire rubber powder.

**Figure 2.** Tire rubber powder at different magnifications: **(a)** without magnification; **(b)** 50× magnification; and **(c)** 100× magnification.

**Figure 3.** Consistency limits for the natural soil ($NR_0P_0$) and various soil–rubber mixtures treated with different PC concentrations: **(a)** liquid limit; **(b)** plasticity index; and **(c)** linear shrinkage.

**Figure 4.** Location of various soil–rubber–PC mix designs on Casagrande's plasticity chart.

**Figure 5.** Standard Proctor compaction curves for the natural soil ($NR_0P_0$) and various soil–rubber mixtures: **(a)** untreated; and **(b)** treated with 0.2 g/l PC.

**Figure 6.** Swell–time curves for the natural soil ($NR_0P_0$) and various soil–rubber mixtures: **(a)** untreated; and **(b)** treated with 0.2 g/l PC.

**Figure 7.** Variations of swelling pressure and swelling potential against rubber content for the tested samples (**H**=*highly expansive*; and **M**=*moderately expansive*).

**Figure 8.** Swell–time characteristics with respect to the oedometer swell test (modified from Soltani et al. (2017[b] and 2018)).

**Figure 9.** Variations of the **(a)** primary and **(b)** secondary swelling rates against rubber content for the tested samples.

**Figure 10.** Variations of the shrinkage and swelling strains, along with corresponding shrink–swell index values, against rubber content for the tested samples ($\mathbf{H^R}$=*highly reactive*; $\mathbf{M^R}$=*moderately reactive*; and $\mathbf{S^R}$=*slightly reactive*).

**Figure 11.** Variations of swelling potential against number of applied wetting–drying cycles for the samples $NR_0P_0$, $NR_{30}P_0$, $NR_0P_{0.2}$ and $NR_{30}P_{0.2}$.

**Figure 12.** Variations of the crack intensity factor, along with corresponding crack reduction factors, against rubber content for the tested samples.

**Figure 13.** Observed crack patterns for the tested samples.

**Figure 14.** Scanning electron micrographs (SEM): **(a)** $NR_0P_0$; **(b)** $NR_{20}P_0$; **(c)** $NR_0P_{0.2}$; and **(d)** $NR_{20}P_{0.2}$.

Accepted manuscript doi:
10.1680/jgein.18.00009

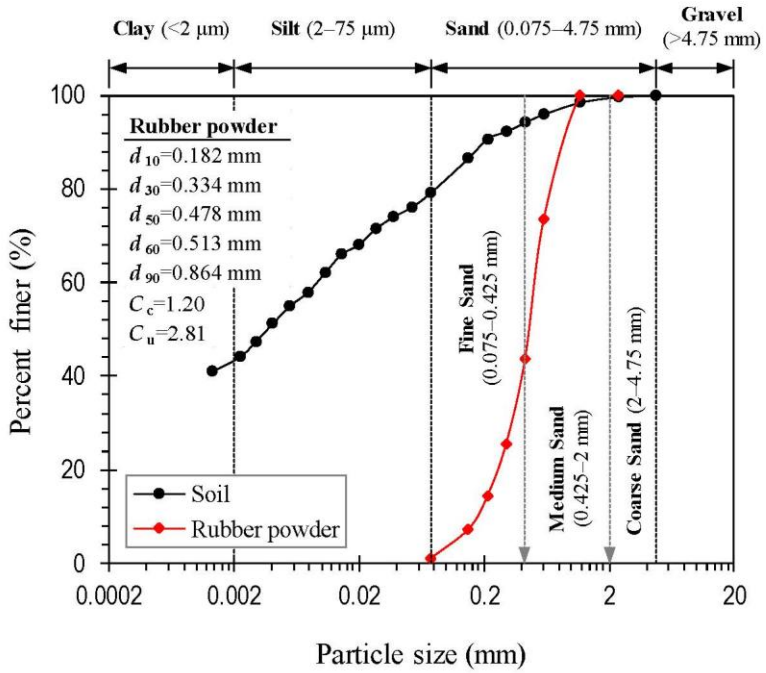


**Figure 1.**

Accepted manuscript doi:
10.1680/jgein.18.00009

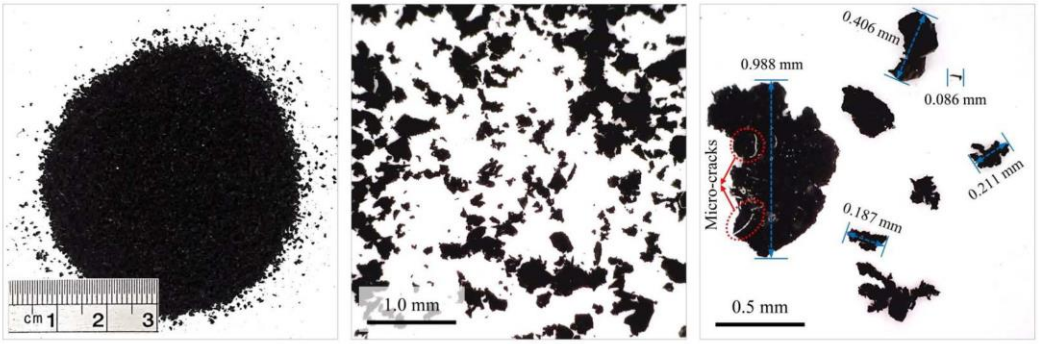


**Figure 2.**

Accepted manuscript doi:
10.1680/jgein.18.00009

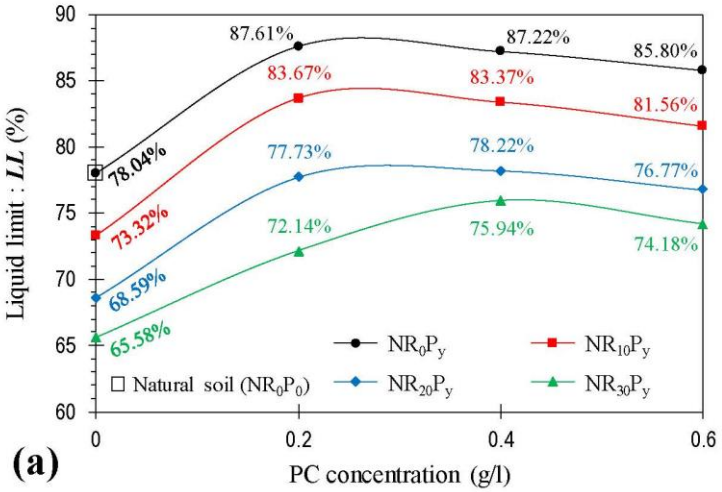


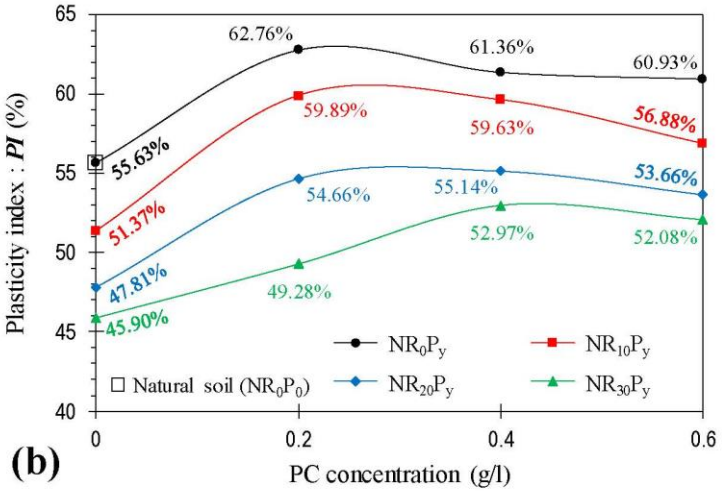


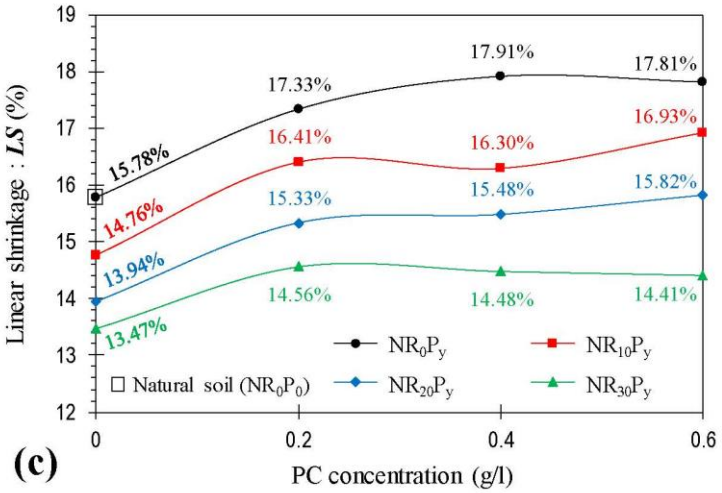


**Figure 3.**

Accepted manuscript doi:
10.1680/jgein.18.00009

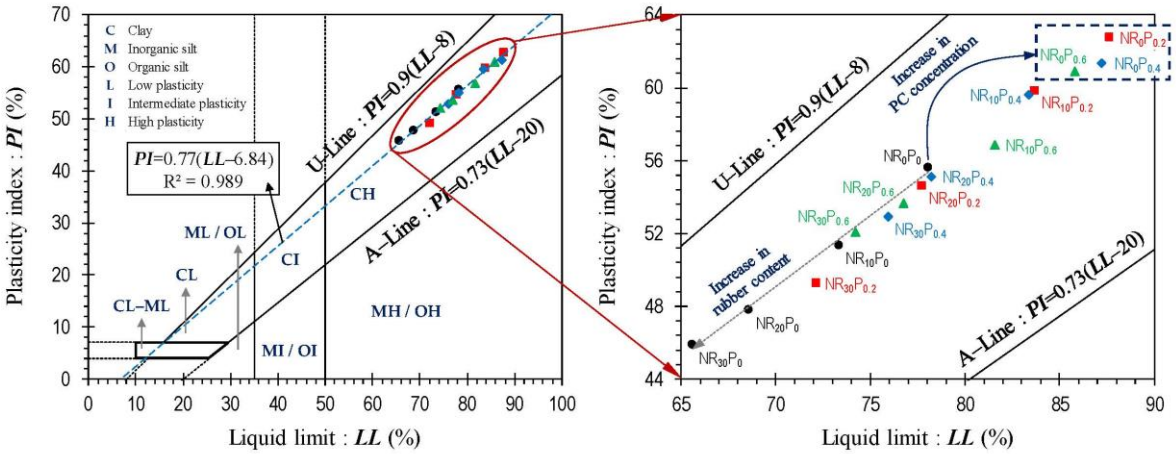


**Figure 4.**

Accepted manuscript doi:
10.1680/jgein.18.00009

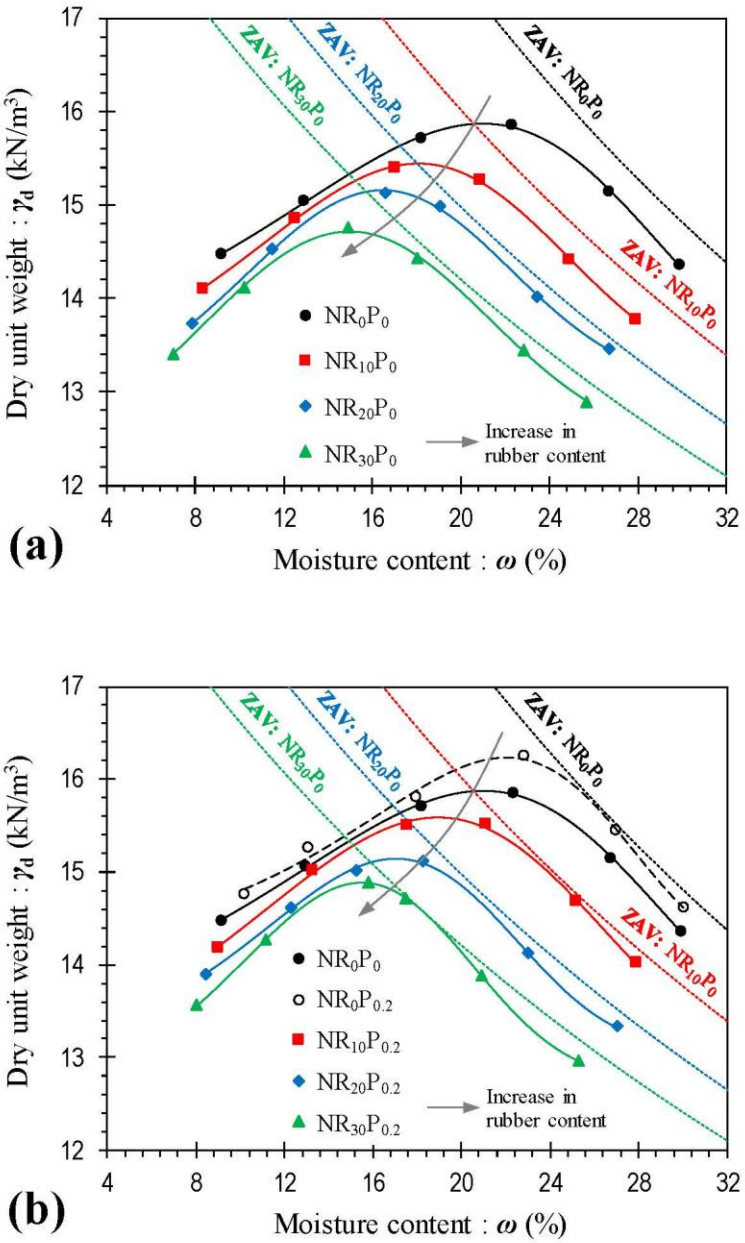


**Figure 5.**

Accepted manuscript doi:
10.1680/jgein.18.00009

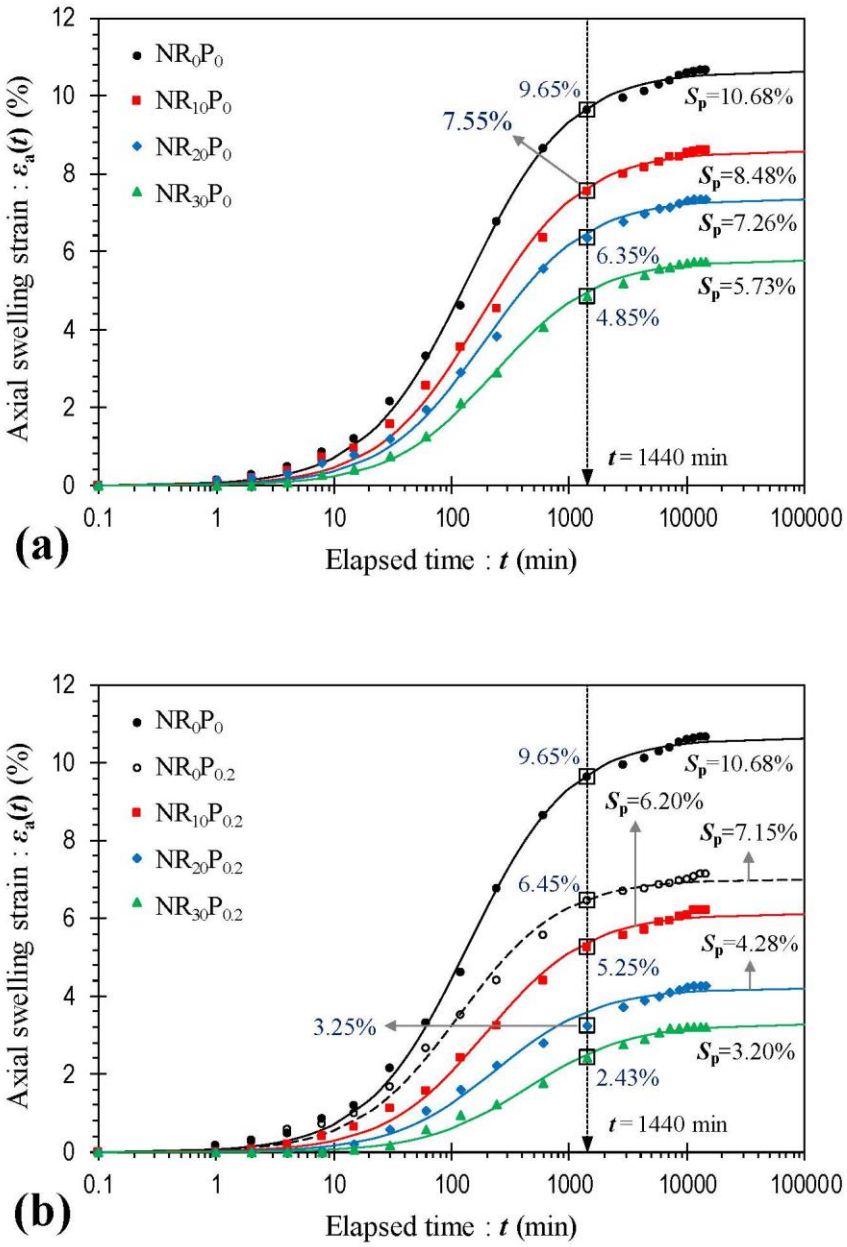


**Figure 6.**

Accepted manuscript doi:
10.1680/jgein.18.00009

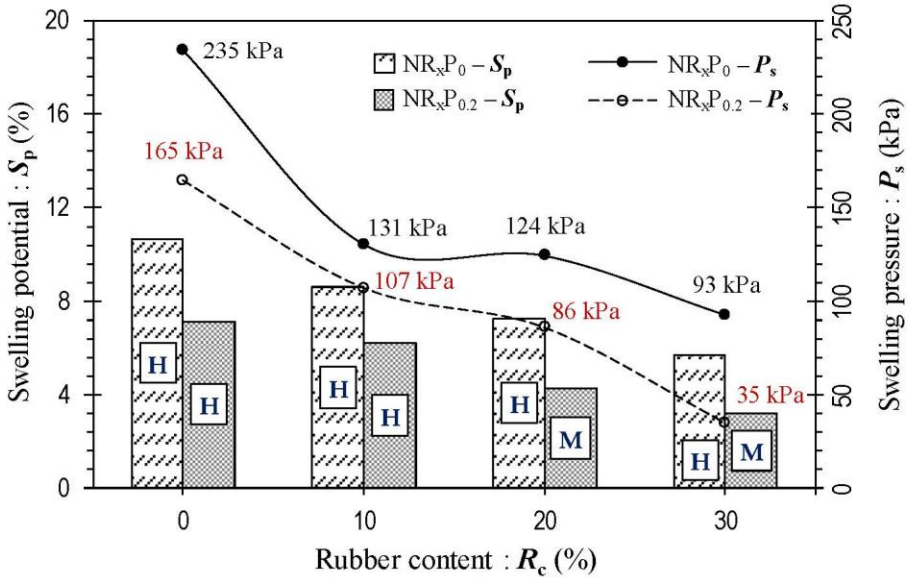


**Figure 7.**

Accepted manuscript doi:
10.1680/jgein.18.00009

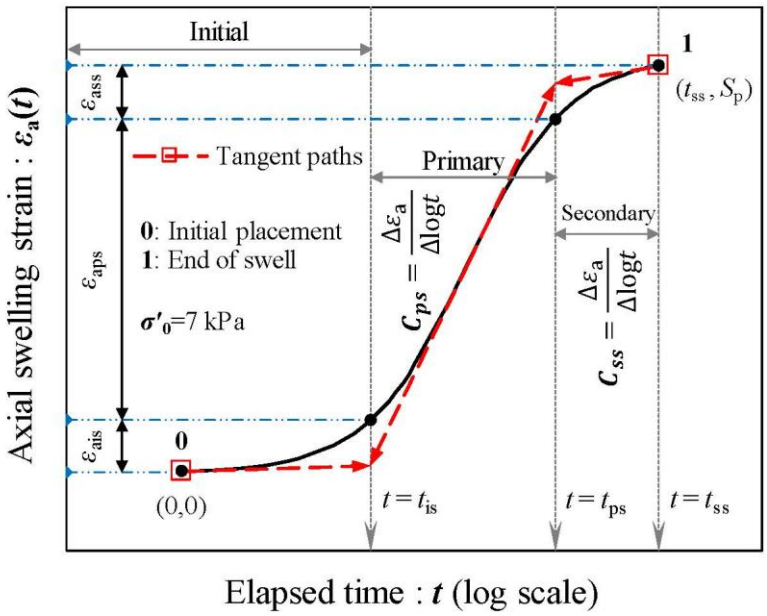


**Figure 8.**

Accepted manuscript doi:
10.1680/jgein.18.00009

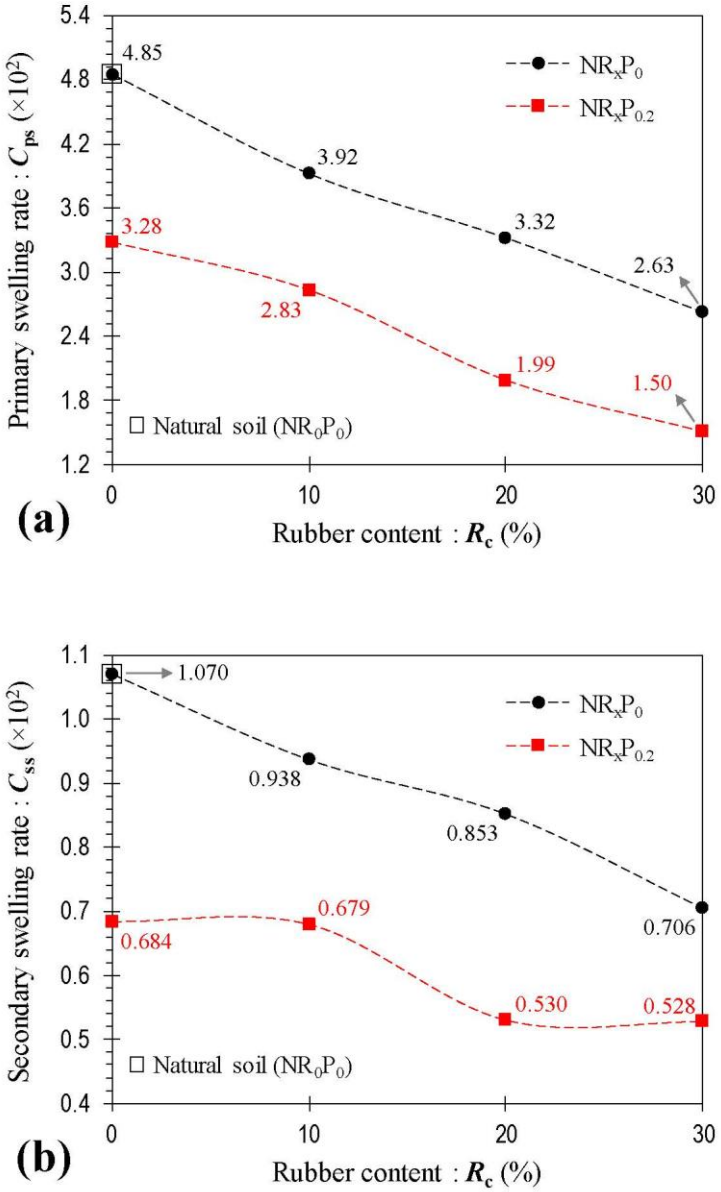


**Figure 9.**

Accepted manuscript doi:
10.1680/jgein.18.00009

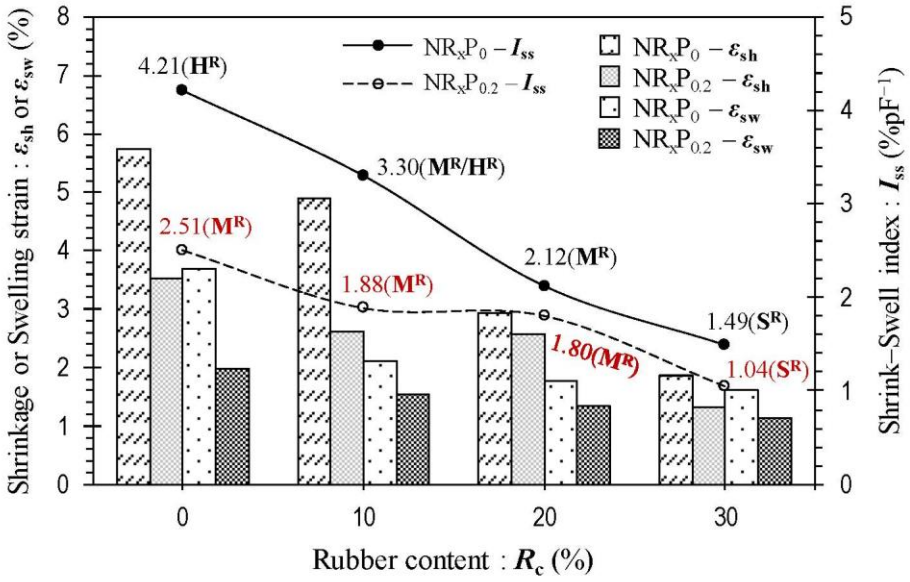


**Figure 10.**

Accepted manuscript doi:
10.1680/jgein.18.00009

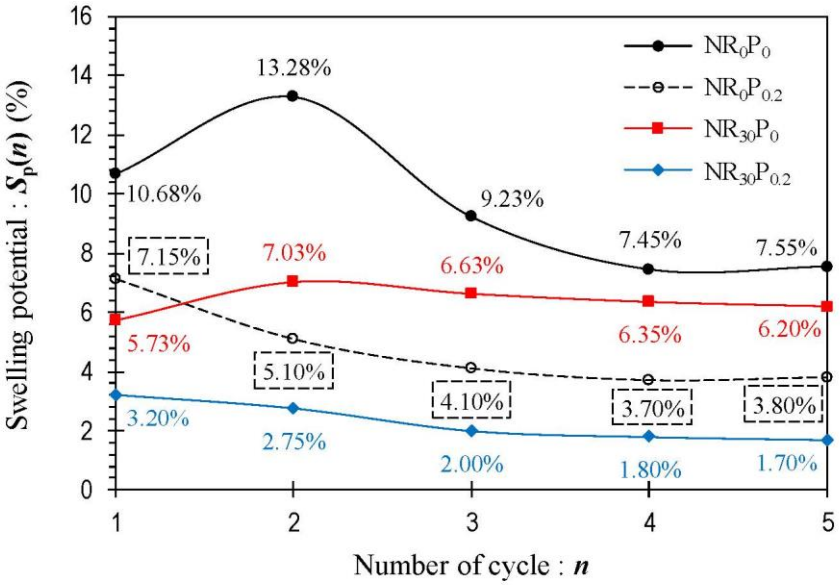


**Figure 11.**

Accepted manuscript doi:
10.1680/jgein.18.00009

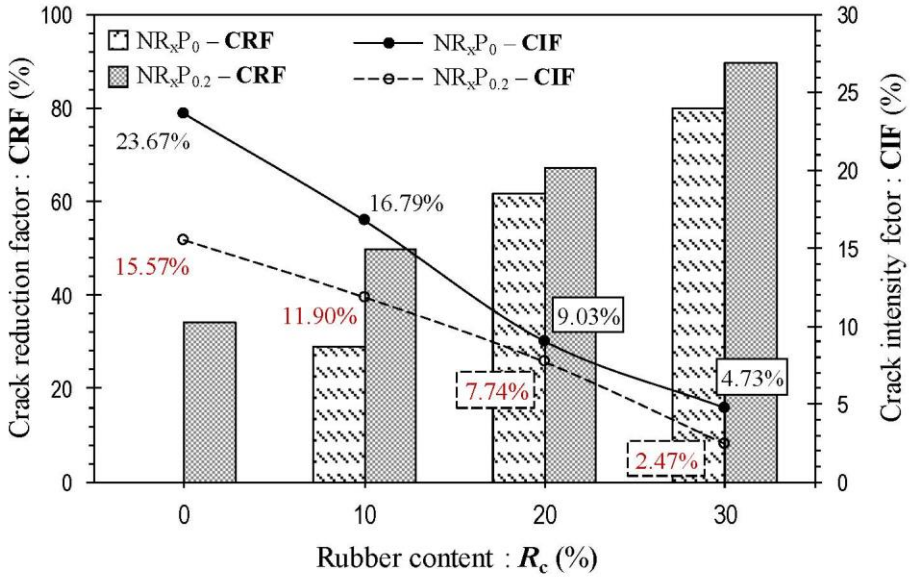


**Figure 12.**

Accepted manuscript doi:
10.1680/jgein.18.00009

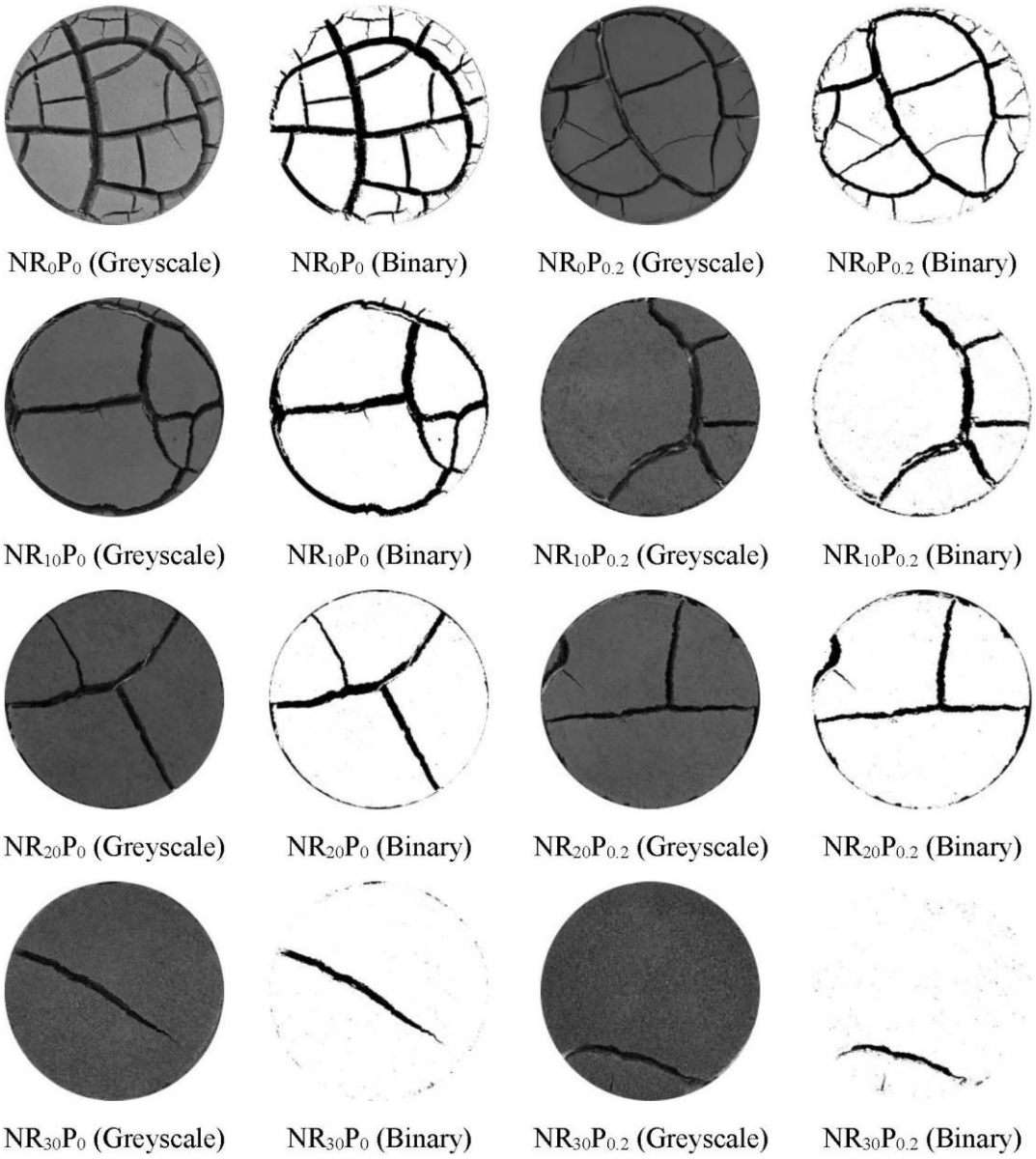


**Figure 13.**

Accepted manuscript doi:
10.1680/jgein.18.00009

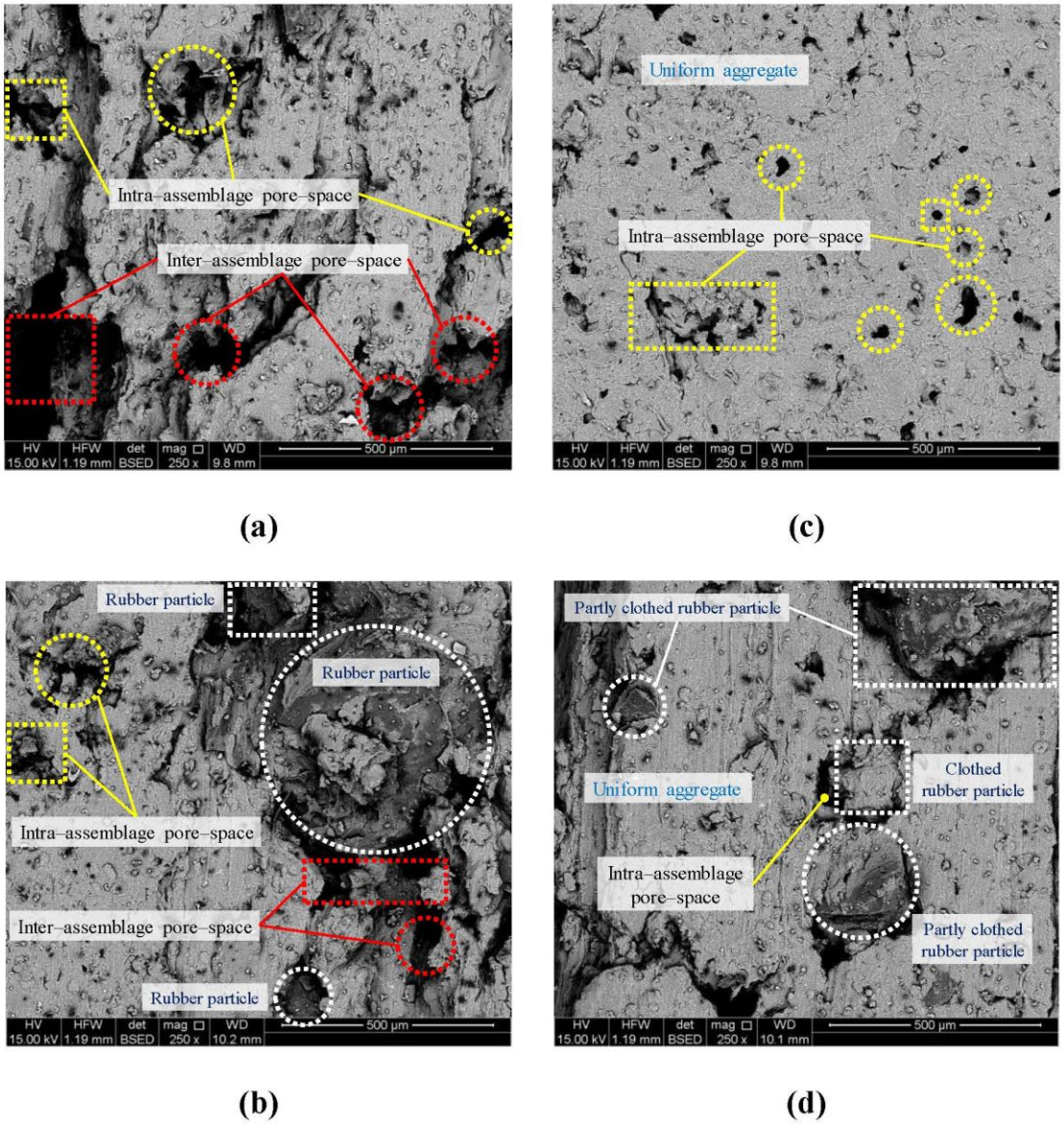


**Figure 14**